School of Chemical and Petroleum Engineering

Department of Chemical Engineering

Preparation and Photocatalysis of Graphite Carbon Nitride Based Photocatalysts

Jijiang He

This thesis is presented for Degree of

Master of Philosophy

of

Curtin University

April 2015

Declaration

To be best of my knowledge and belief this thesis contains no material previously published by any other person except where due acknowledgement has been made. This thesis contains no material which has been accepted for the award of any other degree of diploma in any university.

Signature:  Date: 07-04-2015

Jijiang He

Acknowledgement

I would like to express my deepest gratitude to my supervisor, Professor Shaobin Wang, for his continuous support during my study and research. I could not ask for a better role model, who is inspirational, supportive, and patient. I had no chance to complete this thesis without his encouragement and thoughtful guidance, and it has been an honour to be one of his students.

My deep gratitude must be presented to my co-supervisor, Dr. Hongqi Sun, whose kindness and academic experience have been invaluable to me. I really thank him for paying attention to my study and supporting me to finish my master degree.

I am also grateful to Professor Shaomin Liu, being the chairperson of my thesis, who always encouraged me and supported me morally with great pleasure.

I am also thankful to my colleagues and friends, particularly Dr Guangliang Zhou, Yuxian Wang, Xiaoguan Duan and Stacey Indrawirawan, who have been always helping me on various occasions for my research, given me trainings on various equipment and software.

I am also grateful to all laboratory technical staffs, Karen Haynes, Jason Write, Roshanak Doroushi, Andrew Chan and Xiao Hua, for their great and valuable help to develop the ideas in my research.

I am also thankful to those undergraduate and postgraduate students who have worked with me on this research.

Lastly, and most importantly, a special thank is made to my parents and my brother who supported and encouraged me, both emotionally and financially throughout my degree. I would not have made this far on my study and life in Australia without their immense support.

Publication by author

Referred conference Presentation

Jijiang He, Shizhen Liu, Hongqi Sun, Shaobin Wang, Modification of g-C_3N_4 with metal oxides for high catalytic activity in degradation of methylene blue and phenol, Chemeca 2014, Perth, 28 September - 1 October, 2014

Abstract

Graphitic carbon nitride (g-C_3N_4), possessing an excellent chemical stability and tunable electronic structure, is a potential photocatalytic material. Different strategies have been made to synthesize g-C_3N_4-based photocatalysts with enhanced photocatalytic activities.

The aim of this research is focused on photocatalysis of organic pollution in aqueous solution for water treatment. Metal oxides, polyometalate, and silver silicate modified g-C_3N_4 photocatalysts have been synthesized using hydrothermal and hydrolysis and ion-exchange method. The photocatalysts were characterized by field emission scanning electron microscopy (FESEM), X-ray diffraction (XRD), N_2 sorption isotherms, thermogravimetric analysis (TGA), and UV-vis diffusion reflectance spectroscopy (UV-vis DRS). And the catalytic activities of the photocatalysts were evaluated in decomposition of pollutants, organic dye and phenol, in water. It is demonstrated that modified photocatalysts present better activity than pristine g-C_3N_4.

Content

List of Figures

List of Tables

1

Chapter 1: Introduction

1.1 Motivation

In the modern era, it has been a significant challenge for providing hygiene water for individuals using fresh water for drinking. More than 1000 industrial-origin organic compounds have been detected in different sources of water [1]. A variety of hazardous organic compounds such as pharmaceuticals, surfactants, flame retardants, fragrances, plasticizers and other trace chemicals, which are usually related to human diseases, have been detected in discharged wastewater [2]. Every year, over 2-billion people lack of suitable sanitation facilities in the world, and over 1.2-million die of diseases related to contaminated water in developing countries [3, 4]. Human health therefore has been seriously threatened by the organic pollutants in wastewater.

Natural organic matter (NOM), including microbial secretions and animal waste, and Synthetic organic compounds (SOCs), existence in industrial, agricultural, domestic discharged wastewater, are two mainly sources of organic compounds in wastewater. Compared to NOM, SOCs have been evaluated as the major pollutants in water, over 50% of water pollutants were due to sewage water discharged into rivers and leached into lakes. The major paths of SOCs are involved in pharmaceuticals, surfactants, pigments, flame retardants, steroids, pesticides, food additives and other organic compounds [5-7]. Most of SOCs are toxic that could lead to serious diseases such as cancer, deformity and genic mutation, but some are not or low hazardous, however, they are still harmful [8]. With the more wastewater discharged and organic matter transformation, the higher concentration of toxic SOCs would, more potentially, cause serious human diseases. Over 400 hazardous SOCs have been detected in wastewater, pollutants like toluene, benzene, acetone, phenol and chlorophenols, etc., would pose a great threat to the environment even in a small concentration.

The hazard of water organic pollutants is critical, as most of organic compounds are toxic and hardly self-degradation in nature. A number of studies have been reported that techniques like membrane separation, coagulation, electrochemical process and adsorption could remove SOCs from wastewater effectively [9]. However, issues like economics, secondary pollution and efficiency are limitations of these techniques. Recently, the applications of advanced oxidation processes (AOPs), which involve in a set of chemical

treatment processes by oxidation, such as photocatalysis, supercritical water oxidation and chemical oxidation process, are gaining an attention in wastewater pollutant degradation [10-13]. AOPs have been considered as a low-cost, eco-friendly technique for water remediation.

1.1.1 Photocatalysis of organic pollutant degradation

The photocatalytic process, the combination of heterogeneous catalysis with solar technologies, has been employed as a low-cost, eco-friendly technique of detoxification of wastewater. Various semiconductor photocatalysts have been applied to water purification and a wide variety of undesirable organics have been successfully degraded [14]. In the last decades, TiO_2 is the most widely researched semiconductor photocatalyst, because of its exceptional thermodynamic stability and nontoxicity. However, TiO_2 requires the ultraviolet light or high intensity radiation to drive the photocatalytic process, which limits its practical application. In addition, Photocatalyst separation is one of the challenging issues in water applications. Thus, new photocatalysts, which have high efficiency, easy separation and can be used under low irradiation, are urgently required.

1.1.2 Chemical oxidation of organic pollutant degradation

Chemical oxidation is a remediation technique, which can effectively reduce the concentrations of targeted organic pollutants in water to safe levels. This remediation technique can be used to remediate various SOCs through employing strong chemical oxidizers to oxidize the compounds and change the contaminants into harmless compounds [15].

Permanganate, Fenton's reagent, persulfate and ozone are most commonly used in this process for water remediation. These oxidants are effective and efficient, but still pose many problems. Several catalysts used with these strong oxidants in water treatment may cause secondary pollution [16]. As a consequent, it shows a great potential for modified catalysts for chemical oxidation.

1.1.3 Development of graphitic carbon nitride photocatalysts

Most recently, graphitic carbon nitride (g-C_3N_4) has caught lots of attention, since it is the most stable allotrope of carbon nitride. G-C_3N_4 has similar π-conjugated planar layers like that of graphite, which makes it possess highly stability with thermal and chemical attacks, and an appealing electronic structure [17]. These make it be directly used in sustainable chemistry as a semiconductor catalyst.

G-C_3N_4 has some unique features, such as electronic and optical structure, high photochemical stability, considered as a favourable photocatalyst [18, 19]. G-C_3N_4 had been confirmed to have great performance in photo-degrading organics under visible light irradiation [20], though its efficiency was far from satisfactory.

Worthy mentioning, many compounds and metals could be intercalated into/or fine-tuning the structure and reactivity of g-C_3N_4. Such procedures, such as protonation, boron, fluorine, and sulphur doping, have been used to improve the performance of g-C_3N_4. Most efforts had been made to develop the potential application of g-C_3N_4 as an organic semiconductor in materials and catalysis, and enhance the use by modification in sustainable chemistry [21].

1.2 Aim and objective of thesis

This research aims at the development of graphitic carbon nitride photocatalysts for degradation of organic pollutants in water via photocatalysis and chemical oxidation process.

The following objectives are defined to meet the research goals

i. To investigate the catalytic capacity of graphitic carbon nitride to degrade organic pollutants in aqueous phase.
ii. To synthesize modified g-C_3N_4 photocatalysts for photo-degradation of organic pollutants with UV-Vis light in aqueous phase at room temperature.
iii. To synthesize and develop novel g-C_3N_4 photocatalysts by doping silicates, and evaluate the photocatalytic capacity in aqueous phase.

iv. To investigate the modified catalysts activities for degradation of organic compounds via chemical oxidation process.

1.3 Thesis structure

Chapter 1: This chapter briefly introduced the overall organic pollutants in wastewater that are threatening human and animal health, and presented an overview of two main techniques, photocatalysis and chemical oxidation, for the treatment of wastewater.

Chapter 2: The chapter provided a comprehensive overview of various pollutant removal techniques for the wastewater treatment, particularly on advanced oxidation processes (AOPs), photocatalysis, and the semiconductor materials as photocatalysts. This chapter also briefly presented the sources and health effects of main types of synthesized organic compounds in wastewater.

Chapter 3: This chapter reported the synthesis, characterization, photocatalytic and chemical oxidation properties of modification of g-C_3N_4 with metal oxides (Fe_2O_3-g-C_3N_4, Fe_3O_4-g-C_3N_4 and MnO_2-g-C_3N_4). Synthesis method, characterization, photocatalytic decomposition of methylene blue under UV-vis light irradiation and chemical oxidation of phenol were presented.

Chapter 4: This chapter described the synthesis of polyoxometalate/g-C_3N_4 and its enhanced photodecomposition of organics. The optimum synthesis conditions were discussed. Characterization and photocatalytic decomposition of methylene blue and phenol under UV-vis light irradiation were presented.

Chapter 5: This chapter investigated the synthesis of $Ag_6Si_2O_7$/g-C_3N_4. Photocatalytic activities of the photocatalysts in methylene blue degradation were examined under UV-vis light irradiation. Synthesis method and characterization are also presented.

Chapter 6: This chapter summarized the overall thesis and discussed the performance of all the materials in photodegradation of organic pollutants, and the suggestions for future work.

References

1. Hignite, C. and D.L. Azarnoff, *Drugs and drug metabolites as environmental contaminants: Chlorophenoxyisobutyrate and salicylic acid in sewage water effluent.* Life Sciences, 1977. **20**(2): p. 337-341.

2. Focazio, M.J., et al., *A national reconnaissance for pharmaceuticals and other organic wastewater contaminants in the United States — II) Untreated drinking water sources.* Science of The Total Environment, 2008. **402**(2–3): p. 201-216.

3. Daughton, C.G. and T.A. Ternes, *Pharmaceuticals and Personal Care Products in the Environment: Agents of Subtle Change?* Environmental Health Perspectives, 1999. **107**: p. 907-938.

4. Henriques, J.J. and G.E. Louis, *A decision model for selecting sustainable drinking water supply and greywater reuse systems for developing communities with a case study in Cimahi, Indonesia.* Journal of Environmental Management, 2011. **92**(1): p. 214-222.

5. Kolpin, D.W., et al., *Urban contribution of pharmaceuticals and other organic wastewater contaminants to streams during differing flow conditions.* Science of The Total Environment, 2004. **328**(1–3): p. 119-130.

6. Heberer, T., *Tracking persistent pharmaceutical residues from municipal sewage to drinking water.* Journal of Hydrology, 2002. **266**(3–4): p. 175-189.

7. Barnes, K.K., et al., *Pharmaceuticals and Other Organic Waste Water Contaminants Within a Leachate Plume Downgradient of a Municipal Landfill.* Ground Water Monitoring & Remediation, 2004. **24**(2): p. 119-126.

8. Halling-Sørensen, B., G. Sengeløv, and J. Tjørnelund, *Toxicity of Tetracyclines and Tetracycline Degradation Products to Environmentally Relevant Bacteria, Including*

Selected Tetracycline-Resistant Bacteria. Archives of Environmental Contamination and Toxicology, 2002. **42**(3): p. 263-271.

9. Hamdaoui, O., *Batch study of liquid-phase adsorption of methylene blue using cedar sawdust and crushed brick.* Journal of Hazardous Materials, 2006. **135**(1–3): p. 264-273.

10. Futamura, O., M. Katoh, and K. Takeuchi, *Organic waste water treatment by activated sludge process using integrated type membrane separation.* Desalination, 1994. **98**(1–3): p. 17-25.

11. Bhattacharyya, K.G. and A. Sharma, *Kinetics and thermodynamics of Methylene Blue adsorption on Neem (Azadirachta indica) leaf powder.* Dyes and Pigments, 2005. **65**(1): p. 51-59.

12. Doğan, M., et al., *Kinetics and mechanism of removal of methylene blue by adsorption onto perlite.* Journal of Hazardous Materials, 2004. **109**(1–3): p. 141-148.

13. Yang, Q., et al., *Heterogeneous activation of peroxymonosulfate by supported cobalt catalysts for the degradation of 2,4-dichlorophenol in water: The effect of support, cobalt precursor, and UV radiation.* Applied Catalysis B: Environmental, 2008. **77**(3–4): p. 300-307.

14. Beydoun, D., et al., *Role of Nanoparticles in Photocatalysis.* Journal of Nanoparticle Research, 1999. **1**(4): p. 439-458.

15. Shukla, P., et al., *Nanosized Co3O4/SiO2 for heterogeneous oxidation of phenolic contaminants in waste water.* Separation and Purification Technology, 2011. **77**(2): p. 230-236.

16. Shukla, P., et al., *Cobalt exchanged zeolites for heterogeneous catalytic oxidation of phenol in the presence of peroxymonosulphate.* Applied Catalysis B: Environmental, 2010. **99**(1–2): p. 163-169.

17. Li, X., et al., *Preparation and characterization of graphitic carbon nitride through pyrolysis of melamine.* Applied Physics A, 2009. **94**(2): p. 387-392.

18. Chang, F., et al., *A facile modification of g-C3N4 with enhanced photocatalytic activity for degradation of methylene blue.* Applied Surface Science, 2013. **280**(0): p. 967-974.

19. Song, L., et al., *A metal-free and graphitic carbon nitride sonocatalyst with high sonocatalytic activity for degradation methylene blue.* Chemical Engineering Journal, 2012. **184**(0): p. 256-260.

20. Wang, Y., et al., *Excellent Visible-Light Photocatalysis of Fluorinated Polymeric Carbon Nitride Solids.* Chemistry of Materials, 2010. **22**(18): p. 5119-5121.

21. Wang, Y., X. Wang, and M. Antonietti, *Polymeric Graphitic Carbon Nitride as a Heterogeneous Organocatalyst: From Photochemistry to Multipurpose Catalysis to Sustainable Chemistry.* Angewandte Chemie International Edition, 2012. **51**(1): p. 68-89.

2

Chapter 2: Literature Review

2.1 Introduction

Fresh water shortage has been the greatest challenge in the 21st century; millions of people are consuming water from unprotected sources which contain harmful and toxic organic chemicals. Organic compounds are the majority pollutants in wastewater, while most of them are toxic and seriously threatening the environment and public health. Wastewater is coming from industrial, domestic, agricultural activities, public service and leakage. Among them, industrial and domestic activities, discharging sewage with Synthetic organic compounds (SOCs), are contributing approximately 80% of wastewater. The SOCs such as polycyclic aromatic hydrocarbons (PAHs), polychlorinated biphenyls (PCBs), di-(2-ethyhexyl)-phthalate (DEHP), benzene, phenol and dyes in water discharged by pharmaceutical and chemical industries are not expected, and many methods have been made to control these toxic organic compounds in discharge sewage. Strategies, such as limiting the toxic compounds used, recycling the waste, ameliorating productive processes, and controlling waste treatment processes, have been exploited to reduce the organic pollutants in wastewater.

Basically, the conventionally biological treatment is the most dependable process to decompose the pollutants. However, this treatment process is relatively slow and cannot be employed for some contaminants such as phenol which is not biodegradable. And limitations often appear in terms of high cost and secondary pollution problems in other traditional methods like solvent extraction, and activated carbon adsorption. New techniques such as photodegradation are eco-friendly and cost-efficient. For instance, photodegradation by semiconductor photocatalysis is able to degrade a wide range of organic compounds at normal temperature and pressure without generating any harmful by-product. TiO_2 is one of the most commonly used photocatalysts because of its great photocatalytic capability and nontoxicity. However, TiO_2 is only able to be activated by UV light irradiation ($\lambda<400$ nm), accounting for 4% of sunlight, which is harmful and high energy, and greatly limits practical application. Meanwhile, chemical oxidation is a very effective technique that is used for wastewater remediation to degrade a variety of organic pollutants to carbon dioxide, water and nontoxic inorganics. Nevertheless, toxic metal leaching and harmful by-products are two limitations that cannot be ignored. Therefore, improving the performance of the existing techniques for SOCs treatment processes,

overcoming the limitations of photocatalysis and chemical oxidation, developing novel catalysts and finally increasing their significant efficiency for organics removal are significant ways to convert the wastewater into a usable resource.

2.2 Health effects and sources of synthetic organic compounds

Most of organic compounds are toxic in aqueous phase, and can cause many human diseases like cancer and genic mutation. However, most of them are not intentionally produced; they are emancipated by a series of industrial processes and products decomposition, such as pharmaceutical industry, food processing, metal processing, petroleum industry, paper mills, and plastic industries. The major toxic SOCs are polycyclic aromatic hydrocarbons (PAHs), polychlorinated biphenyls (PCBs), di-(2-ethyhexyl)-phthalate (DEHP), benzene, phenols, and dyes, and the detail of them are described as follows:

Polycyclic aromatic hydrocarbons (PAHs) are presented in fossil fuels, which means PAHs are emitted into atmosphere during the carbon-contain fuels combustion and waste incineration. Oil spills are another major cause of PAHs released. In addition, PAHs dyes are widely produced, used, and discharged into water every year. PAHs can enter the food chain through aqueous organisms, and even low concentration of PAHs can poison fish. And children exposure to PAHs would affect their IQ development and lead to childhood asthma.

Polychlorinated biphenyls (PCBs) are synthetic organic compounds, and are used commercially. PCBS are widely used as dielectric and coolant fluids in major industry areas, such as in electrical appliances, cutting fluids for machinery operations, and cooling agents in heat transfer systems [1].

PCBs are stable compounds with a long life (more than 8 years) in natural environment and have environmental toxicity; PCBs have been defined as a persistent organic pollutant [2]. According to recent research, PCBs can be adsorbed in the hydrosphere and accumulate in the organic fraction of soils [3]. The toxicity of PCBs is affecting the water, soil, and food. People and animals can be exposed to PCBs through consuming contaminated air, food, and skin contact with polluted water. Once exposed, some chemicals inside the organism would be changed by PCBs.

Di-(2-ethyhexyl)-phthalate (DEHP) is widely used as a plasticizer in cosmetics, children's toy, shampoos, building materials, automobiles, and polyvinyl chloride (PVC) products [4]. DEHP is being a widespread organic pollutant with significant human exposure [5], and the acute toxicity of DEHP is seriously threatening animal and human health, such as disruption of the endocrine system [6, 7]. DEHP can be present in food and water, and it can also leach into a liquid that contacts with the plastic, especially the wastewater produced from PVC industry.

Benzene is one of the most elementary petrochemicals, and is widely used as an industrial feedstock and as a solvent. Benzene is used for printing and lithography, paint, rubber, adhesives and coatings, detergents, extraction and rectification. Human exposure to benzene is a global health problem. Benzene increases the risk of cancer and targets human organs. Water and soil contamination are important pathways of concern for transmission of benzene, while the major sources of benzene in water are discharged from factories, and leaching from gas storage tanks and landfills.

Phenols, sometimes called phenolics are produced in a large scale in worldwide now. Phenolic compounds are significant raw materials and intermediates for industrial purposes, such as laboratory processes, chemical industry, chemical engineering processes, wood processing and plastics processing [8-10]. Due to their toxicity and wide use, phenolic compounds are universal pollutants that are discharged to natural water system and wastewater from the industrial processes. Moreover, phenols are also released from vehicle emission, cigarette smoking and bushfire [11]. The exposure from phenols may induce corrosive effect to the eyes, skin and respiratory tract [12]. Repeated or prolonged contact to phenols may cause harmful effects on the central nervous system.

Dyes are colored substances which have an affinity towards the substrate being applied. Most of commercial dyes are ionic and aromatic organic compounds [13-15]. Many industrial processes, including textile, paper, printing, food, cosmetic and plastic industries, are using dyes to color their products [14, 16, 17]. The dyes are generally used in an aqueous solution, which means wastewater is the major route where the dyes are released into the environment. The huge amount of contaminated water was generated by the substantial dyeing processes. Dyes in the water are not safe, and pleasant. Some dyes even

would cause some harmful effects such as increased heart rate, vomiting, shock, cyanosis, jaundice and tissue necrosis in humans [13].

In summary, most of major synthetic organic compounds are classes of aromatic organic compounds and have similar structural, chemical properties and toxicities. These organic compounds are universal and can be difficult to be degraded by natural processes. Among these SOCs, phenol is produced naturally, synthesized artificially, and applied widely, and dyes are commercially used and widely present in wastewater, so phenol and dyes are ideal model compounds for wastewater treatment study.

2.3 Wet air oxidation (WAO)

Wet air oxidation (WAO) is a commonly used technology that is applied in wastewater treatment. The WAO technology has been used commercially since 1950s, and currently there are over 200 plants using this process for treating wastewater around the world. WAO is a hydrothermal treatment that involves wastewater treatment at high temperature and pressure using air or pure oxygen as an oxidant [18, 19]. During the process, toxic organic compounds which have high molecular chain split to lower molecular compounds such as formic acid, carboxylic acid, acetic acid, and subsequently decomposed into water and carbon dioxide. Based on mechanistic reactions, the reaction mechanisms in parallel are shown in the following equations [20].

1) Direct oxidation of organic compounds to carbon dioxide

$$\mathrm{R-H} + O_2 \xrightarrow{k_1} CO_2$$

2) Oxidation of organic compounds with intermediate compounds

$$\mathrm{R-H} + O_2 \xrightarrow{k_2} CH_3COOH \xrightarrow{k_3} CO_2$$

The kinetic equation obtained from two reaction schemes above is given below[19].

$$\frac{(\mathrm{R-H} + CH_3COOH)}{(\mathrm{R-H} + CH_3COOH)_0} = \frac{k_2}{k_1+k_2-k_3}\mathrm{e}^{-k_3 t} + \frac{k_1-k_3}{k_1+k_2-k_3}e^{-(k_1+k_2)t}$$

The sequence of the oxidation of organic compounds and the formation of radical reaction could be divided into 3 stages: initiation, propagation and termination. These stages are shown in the following equations [21].

Initiation $\mathrm{R-H} + O_2 \rightarrow R^{\cdot} + \mathrm{H}O_2^{\cdot}$

Propagation $R^{\cdot} + O_2 \rightarrow \mathrm{R}O_2^{\cdot}$

$\mathrm{R-H} + \mathrm{R}O_2^{\cdot} \rightarrow \mathrm{ROOH} + R^{\cdot}$

Termination $\mathrm{R}O_2^{\cdot} + \mathrm{R}O_2^{\cdot} \rightarrow \mathrm{ROOR} + R^{\cdot}$

In this process, organic compounds in wastewater will be oxidized by oxygen. The operations are commonly at high temperature (120 – 320 ℃) and pressure (0.2 – 20 MPa). In order to achieve the optimum results, WAO is preferred at chemical oxygen demand ranges from 20,000 to 200,000 mg/L, and can easily reach 95-99% conversion of toxic organics [22]. However, this technique is generally not able to decompose wastewater completely into water and carbon dioxide. Therefore, WAO usually requires additional biological treatment processes to meet the requirements for waste disposal into the environment.

A WAO plant comprises a high-pressure feeding pump, an air compressor, a heat exchanger, a co-current bubble column reactor and a vertical column separator [18]. The basic process flow sheet of WAO plant can be seen in Figure 2.1. The waste is fed by a high-pressure pump through a heat exchanger to the reactor constantly. While the air compressor is giving air or oxygen, and the waste is combined with oxidation in the mixing point. After heating through a heat exchanger, the fluid reaches the reactor and the exothermic reaction takes place. After the reaction, the effluent flows through to the separator and is separated into gas and liquid, then disposed into the environment after a post-treatment by an addition biological facility.

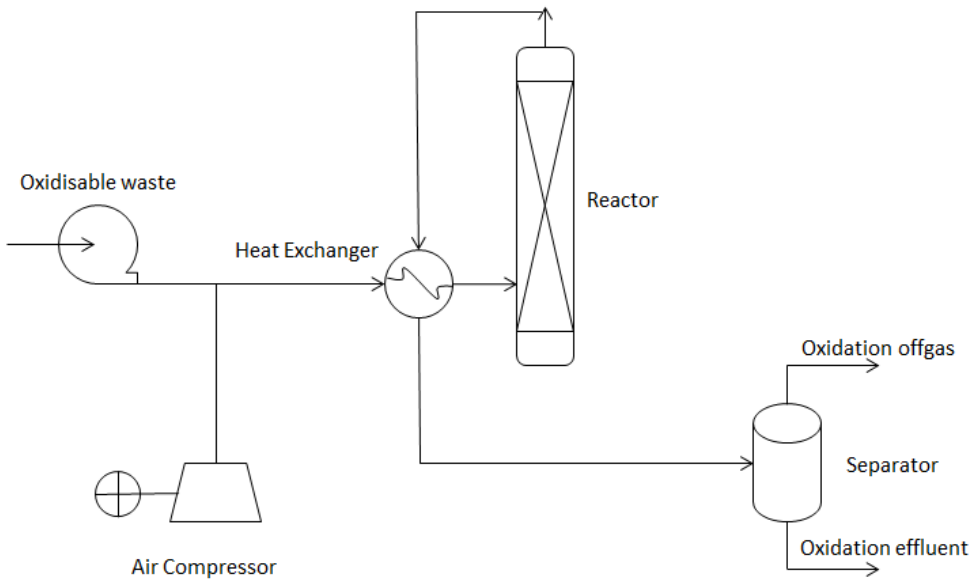

Figure 2.1 Basic treatment system of WAO plant

In general, WAO is successful to decompose various kinds of organic compounds in wastewater. Table 2.1 shows the results of a variety of organic compounds which were degraded using WAO processes [20, 23-28].

Table 2.1 Wet air oxidation of various organic compounds.

compounds	**Treatment temperature (℃)**	**Treatment pressure (MPa)**
Acetic Acid	265-300	2-20
Acetonitrile	255-320	1
Acetone	160-260	6.8-13.6
Alkylbenzen sulfonate	200-240	1.5
Ammonium thiocyanate	225-250	2-15
Black liquor	187-257	0.21

Butyric Acid	237-257	6.8-13.6
Cyanide	225-250	2-15
Diethanolamine	140-240	0.39-1.38
Fuel-oil	200-350	20
Formic Acid	300	1
Glucose	177-265	10.9
Morpholine	150-240	0.39-1.38
Nitriteacetic Acid	200-225	5-15.2
Oxalic Acid	207-288	2-20
phenol	150-180	0.3-1.15
Propionic Acid	180-315	7-13
Sec-butanol	160-200	6.8-13.6
Tetrachloro ethylene	225	13.8
Tert-butyl alcohol	220	3

The significant drawbacks of wet air oxidation are the high costs of the process of compressed air and waste pumping continually. In addition, noble metal catalysts, used for the process is relatively expensive. The most economical condition of WAO is the concentration of an oxidant in 1-20% by weight with water; because the materials would reach with oxidants to generate sufficient heat to keep the operation temperature and pressure to the desired conditions in the reactor and without external power source [28].

2.4 Catalytic Wet Air Oxidation (CWAO)

Due to the disadvantages of WAO, especially hardly to completely remove organic pollutants, Catalytic Wet Air Oxidation (CWAO) technology has been developed to reach the zero discharge. In fact, the zero discharge is possible to achieve because a catalyst can convert the intermediate products like acetate acid and ammonia, which are hard to convert without using a catalyst, into carbon dioxide and water. There are several advantages of CWAO, such as low power requirements, reduced gas release and low operation conditions [29]. With the continually developed, the typical operating conditions of CWAO are at a temperature 80-180 ℃ and a pressure of 1-5 MPa [30].

A CWAO plant consists of a column reactor, a booster pump, an air compressor, a heat exchanger and a liquid-gas separator. The basic flow sheet can be seen in Figure 2.2. Air compressor is giving air as an oxidant the mixing with the wastewater and passes through a catalyst at operating temperature and pressure. After reaction, the effluent was cooled through the heat exchanger to the liquid-gas separator. A separator is used to separate the effluent into gas and liquid. The treated gas and water would be released to the environment [31].

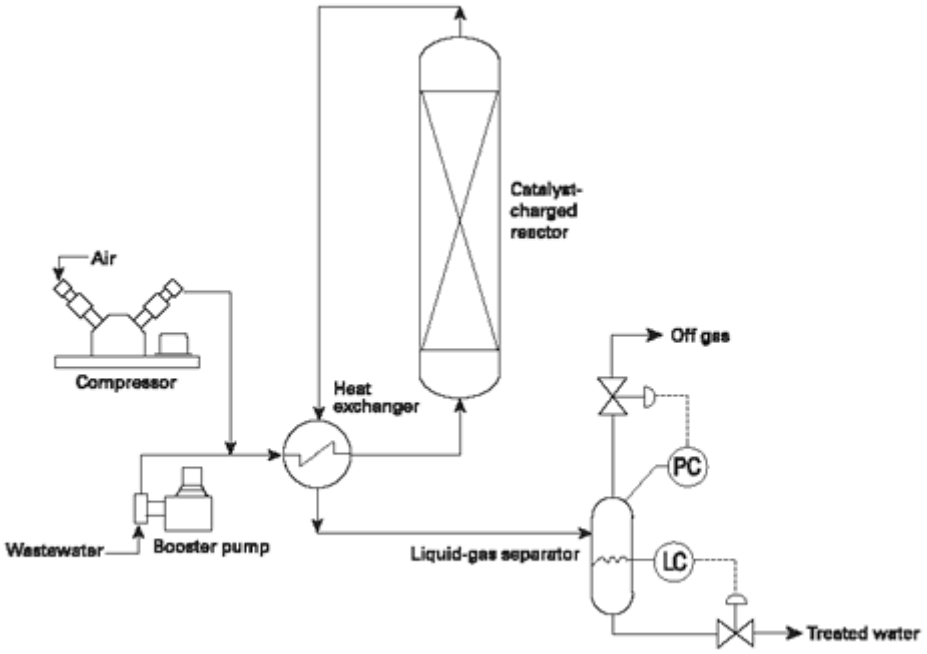

Figure 2.2 A basic flow of Catalytic Wet Air Oxidation.

In CWAO, the catalytic agents are made up of three main classifications: noble metal, metal oxide and metal salts [32]. Metal salts, which are known as homogeneous catalysts, are relatively more efficient compared to heterogeneous catalysts. However, homogeneous catalysts in system are another pollution problem in the water and needs a more process for separation of the catalysts. In addition, most of dissolved metal catalysts are detrimental to the environment so that it is not easy to achieve the separation economically or technically [33]. By contrast, heterogeneous catalysts are easily recoverable and reusable, and high energy efficiency [34, 35]. Nevertheless, heterogeneous catalytic oxidations have some limitations related to chemical and physical stabilities of catalysts such as leaching, catalyst deactivation and catalyst damage.

In the oxidation process, several characteristics of a catalyst for liquid-phase oxidation must meet to be used in industry [36];

1) Exhibiting high oxidation rate or activity.
2) No poisoning and stability in extended use at raising temperature.
3) Mechanical stability and resistance to attrition.
4) Unique in most cases.
5) Chemical and physical stabilities in different conditions.

There are 5 steps in heterogeneous catalysis involved in reactions [37];

1) Diffusion of the reactants on the catalyst surface.
2) Adsorption of reactants to the catalyst surface.
3) The reaction on the catalyst surface.
4) Desorption of products from the catalyst surface.
5) Diffusion of products from the catalyst surface.

In the most catalytic reactions, reaction kinetics is based on the molecular transport (adsorption and diffusion) rather than reaction itself. Therefore, the development and modification of catalysts are needed. The catalyst directly activates pollutant molecules, advances their disintegration into radicals. The catalytic cycle of pollutant oxidation is related to the reduction-oxidation reaction as shown below [38].

$$ROOH + Me^{(n-1)+} \rightarrow RO^{\cdot} + Me^{n+} + OH^{-}$$

$$ROOH + Me^{n+} \rightarrow RO_2^{\cdot} + Me^{(n-1)+} + H^+$$

The metal catalysts that are applied in CWAO technique are generally a noble metal including Pd, Pt, Ir,Rh and Ru [32], which have been valid in the treatment of various pollutants such as phenol, acetic acid, ammonia, carboxylic acid, Kraft effluents, olive oil mill wastewater etc.[38-45]. The CWAO of organic pollutants using noble catalysts are summarized in Table 2.2.

Table 2.2 Summary of CWAO of organic pollutants using different noble metals.

Noble Metal	**Support**	**Pollutant**	**T (℃)**	**P (MPa)**
Ru	TiO_2	Succinic Acid	55-250	0-1.0
Ru	ZrO_2, C, AC	Kraft effluent	140	2.0
Ru	CeO_2	Maleic Acid	160	2.0
Ru, Ir, Pd, Ag	CeO_2, ZrO_2-CeO_2	Acetic Acid	200	2.0
Pt	C	Carboxylic Acid	150	0.2
Pt	γ-Al_2O_3	phenol	155-200	5.05
Pt	γ-Al_2O_3	Acetic Acid	180	2.0
Pt-Ag	MnO_2-CeO_2	Phenol	120	0.5
Pt, Pb, Ru, Rh	CeO_2	Ammonia	180	2.0
Pt, Ru, Rh	TiO_2, CeO_2, C	Phenol / Acrylic Acid	170	2.0
Pd	C	Ammonia	280	2.0
Ir	C	Butiric Acid	200	0.69
Ir	CeO_2, TiO_2, C	Ammonia	180	1.5

Among the noble metal catalysts employed for the CWAO, the ability of oxidation in the process is relying on the pollutants. For instance, the catalytic activity order of oxidation of acetic acid is Ru > Ir > Pd[46]. With p-chlorophenol, catalytic activity increases in the order Ru < Pd <Pt [47]. While in the oxidation of polyethylene glycol, the removal capability of noble metals follows Ru = Rh = Pt > Ir >Pd [48].

A pure form or the mixed metal oxides is another type of catalysts employed in CWAO. Metal oxide catalysts are mainly including one or several of Cu, Mn, Co, Cr, Ti, Ni, Bi, Zn, Al and other metals. Copper oxide is widely used for the liquid effluent oxidation. The catalyst with copper and alumina support is successfully oxidizing phenol [49, 50]. Formic acid has been successfully oxidized using another commercial catalyst, Cu/ZnO [51]. The other commercial catalysts are relatively effective to decomposition phenol and substituted phenolic compounds. In the phenol oxidation, catalytic activity of metal oxides was shown with the following order [52]:

$CuO > CoO > Cr_2O_3 > NiO > MnO_2 > Fe_2O_3 > YO_2 > Cd_2O_3 > ZnO > TiO_2 > Bi_2O_3$

Several tests on the CWAO of organic pollutants over different metal oxide catalysts [53-75] are shown in Table 2.3.

Table 2.3 Metal oxide catalysts based on CWAO.

Metal oxide	**Support**	**Pollutant**	**T (℃)**	**P (MPa)**
Cu, Ni, Co, Fe, Mn	γ-Al_2O_3	phenol	150	5.05
Cu	MCM-41	phenol	150	2.0
CeO_2	γ-Al_2O_3	phenol	180	0.5-2.0
CeO_2	-	phenol	95-180	0.5-1.0
Fe	AC	phenol	100-127	0.8
Cu, Cr	-	phenol	127-150	0.32
Cu, Cr, Ba, Al	-	phenol	127	0.8

Cu	γ-Al_2O_3	phenol	140	0.9
Cu, Zn, Co	-	phenol	130-180	0.73
Cu, Zn	γ-Al_2O_3	phenol	105-150	0.15-0.8
Mn, CeO_2	-	phenol	110	0.5
Mn, Co	-	phenol	170	1.3
Cu	AC	phenol	160	2.6
Mn, Co	-	p-chlorophenol	170	1.3
Cu, Zn	γ-Al_2O_3	p-chlorophenol	105	0.15-0.5
Cu, Zn	-	Formic acid	200	4
Fe	-	Acetic acid	252	6.7
Cu, Mn, La	ZnO, γ-Al_2O_3	Acetic acid	250	1.0
MnO, CeO	-	Ammonia	263	1.0
MnO_2, CeO_2	-	Alcohol distillery	180	0.5

Activated carbon is another type of catalyst used in CWAO. The high surface area of activated carbon makes them have a very good performance in the oxidation process. In addition, the condition of using activated carbon as a catalyst in CWAO processes should be set at a mild condition (temperature less than 150 °C and pressure at 10 atm)[76]. Among the most catalysts, activated carbon is a less expensive alternative to degrade phenolic compounds.

2.5 Advance Oxidation Process (AOP)

Advance oxidation processes (AOPs) are a set of chemical treatment procedures designing to decompose organics in water by highly reactive species, such as hydroxyl radicals and sulphate radicals [35, 77, 78]. Hydroxyl radicals has an extremely high standard oxidation potential, so once hydroxyl radicals are generated and pollutants would be rapidly, efficiently and unselectively converted into small inorganic molecules. The mechanism can be seen below.

$$C_aH_BX + mOH \rightarrow aCO_2 + \frac{b}{2}H_2O + X^{n-}$$

Recently, several oxidants, mostly a sulphate based oxidants, are proposed as an alternative to hydroxyl radical for applications in AOPs [79, 80]. And other optional ways for combination of the wastewater treatment are as follows.

2.5.1 Chemical Oxidation

Chemical oxidation is a technique that uses reagents to transform, degrade, or oxidize organic compounds in wastewater into harmless components. This technique has been used for decades for remediation of groundwater and in the wastewater industry for the treatment of organic pollutants. The chemical compounds used in wastewater treatment are served as the oxidants, and the ability of the oxidation of the oxidants against pollutants in the wastewater is influenced by redox potential of each oxidant. The standard redox potential of some oxidants is shown in Table 2.4 [81].

Table 2.4 Redox potential of oxidants.

Oxidants	**Redox potential E◦ (eV)**
Fluorine	3.03
Hydroxyl radical	2.70

Sulphate radical	2.60
Atomic oxygen	2.42
Ozone	2.07
Persulphate	2.01
Hydrogen peroxide	1.78
Permanganate	1.68
Chlorine dioxide	1.57
Hypochlorous acid	1.47
Chlorine	1.36

The oxidants including chlorine, permanganate, peroxide, persulphate and ozone have been widely used in wastewater treatment. Chlorine is usually employed in drinking water treatment because it can destroy the pathogenic organisms in water. Nevertheless, chorine can only be used for mild oxidation process by selective chemicals, and the use of chorine in high concentrations of contaminants would advance the formation of detrimental intermediate compounds [82].

Potassium permanganate is another significant oxidant used in wastewater treatment for color, taste and odor problems. In the water, potassium permanganate would generate several types of active radicals, which react and turn contaminants into harmless components [83]. The different types of active radicals are generated based on the reaction condition such as pH.

$$MnO_4^- \overset{H^+}{\leftrightarrow} HMnO_4 \overset{H+}{\leftrightarrow} H_2MnO_4 \overset{-H_2O}{\longleftrightarrow} MnO_3^+$$

Some studies showed the oxidation of alkyl benzene at pH higher than 2.5, MnO_4^- will dominated the oxidation process, while $HMnO_4$ will be the major active radical at a pH

lower than 0.3[84, 85]. The drawback of using permanganate as an oxidant is the precipitation in the end products which needs additional separation processes.

Potassium peroxydisulphate, known as persulphate, is generally used in the processing of underground water [86]. Potassium peroxydisulphate can generate highly active sulphate radicals and has a great oxidation capacity in a large range of pH [87].

$$S_2O_8^- \xrightarrow{thermal} 2SO_4^{2-}$$

Persulphate ion can be generated to sulphate radicals with the existence of divalent metal ion such as Fe^{2+} ions, the equation can be seen as below [86].

$$S_2O_8^- + Fe^{2+} \rightarrow SO_4^{\cdot -} + Fe^{3+} + SO_4^{2-}$$

The process of ozone in the water treatment is transporting ozone to the bottom of the wastewater, and the formation of ozone transfer to oxygen, while the solubility of ozone is 12 times more than oxygen [88]. The biggest advantage in using ozone as an oxidant is that ozone does not leave any residual chemical which requires additional removal process. The processes of ozonation can occur directly with ozone molecules or indirectly through the formation of hydroxyl radicals, and then only leaving behind oxygen [89].

$$3O_3 + OH^- + H^+ \rightarrow 2OH^{\cdot} + 4O_2$$

Ozone can react with a variety of important environmental pollutants; however, it also reacts with many other substances such as minerals which are not the targeted substances.

2.5.2 Fenton processes

Fenton's reagent treatment is a classically reactive system involving the addition of hydrogen peroxide and iron ion in the wastewater [90]. Many studies reported that Fenton's reagent is effective in degrading toxic organic pollutants such as alcohol, phenols, chlorophenol, benzene, trichloroethylene, and tetrachloroethylene.

In Fenton processes, the Fe^{2+} is oxidized by hydrogen peroxide to Fe^{3+}, while, the reduction of ferric iron (III) to ferrous iron (II) happens at pH 2.7-2.8 [91]. Hydroxyl radicals generated

by the Fenton's reagent is simple and effective, which does not need any special reactants or apparatus. And studies have reported that the iron in this oxidative system is non-toxic, and hydrogen peroxide is eco-friendly and easy to handle.

The following is the complete reactions of Fenton chemistry [92]:

$$Fe^{2+} + H_2O_2 \rightarrow Fe^{3+} + OH^- + OH^{\cdot}$$

$$Fe^{3+} + H_2O_2 \rightarrow H^+ + Fe^{2+} + OOH^{\cdot}$$

$$OH^{\cdot} + H_2O_2 \rightarrow H^+ + Fe^{3+} + HOO^{\cdot}$$

$$OH^{\cdot} + Fe^{2+} \rightarrow Fe^{3+} + OH^-$$

$$Fe^{3+} + HOO^{\cdot} \rightarrow Fe^{2+} + HOO^+$$

$$Fe^{2+} + HOO^{\cdot} + H^+ \rightarrow Fe^{3+}H_2O_2$$

$$HOO^{\cdot} + HOO^{\cdot} \rightarrow H_2O_2 + O_2$$

The free radicals generated will be engaged in secondary reactions, and these reactions occur simultaneously.

Fenton oxidation reaction is effective; however, this process has some limitations, such as the ratios of Fe^{2+}/H_2O_2, which affect the rate of hydroxyl radicals reacting with the pollutants. Thus, lots of research has been done to develop the Fenton catalysts. In order to enlarge the specific surface area, carbon nanotubes (CNTs) have been used as supports in synthesis of catalysts [93-95]. The performance of Fe_2O_3 / CNTs is enhanced in phenol degradation. Activated carbon (AC), which has outstanding mechanical strength and porous structures, is also used to support Fe in organic pollutant decomposition [96-98]. And new types of carbon material such as graphene, graphene oxide have been proven that they will improve organic degradation as catalyst supports [99, 100].

Meantime, iron based catalysts, such as zero-valent iron (ZVI or Fe^0) and Fe_3O_4 have recently developed in Fenton-like system. ZVI in wastewater can facilitate the decomposition of toxic contaminants [101-104]. The reactions can be seen as follow:

$$Fe^0 \rightarrow Fe^{2+} + 2e^-$$

$$contaminant + ne^- \rightarrow X + H_2O$$

To conclude, Fenton's reagent is a simple, effective and environment-friendly water treatment system. The efficiency of reaction systems can be improved by adding adequate oxidants. Thus, Fenton processes are reasonable for the remediation of wastewater.

2.5.3 UV/Oxidant system

Free radicals such as hydroxyl or sulphate radicals would be also generated by UV light irradiation. Photochemical oxidation is often used for the wastewater treatment that has low chemical oxygen demand (COD). The three stages of the process include initiation, propagation and termination [105], which can be seen below.

Initiation stage

$$H_2O_2 + hv \rightarrow 2OH^{\cdot}$$

Propagation stage

$$H_2O_2 + OH^{\cdot} \rightarrow HO_2^{\cdot} + H_2O$$

$$H_2O_2 + HO_2^{\cdot} \rightarrow OH^{\cdot} + H_2O + O_2$$

$$HO_2^- + HO_2^{\cdot} \rightarrow OH^{\cdot} + OH^- + O_2$$

Termination stage

$$OH^{\cdot} + HO_2^{\cdot} \rightarrow H_2O + O_2$$

$$OH^{\cdot} + OH^{\cdot} \rightarrow H_2O_2$$

This process uses H_2O_2 as an oxidant to achieve the optimal generation of hydroxyl radicals. Several studies reported that various organic pollutants such as phenol, chlorophenol, nitro benzene, and hydroxyl phenyl acetic acid have been successfully oxidized [106-108].

Another combination is ozone with the UV irradiation. UV/O_3 system has been widely used in the remediation of wastewater especially for the industrial effluent. In general, ozone is

injected into wastewater until saturated, then wastewater solution irradiated by UV-light [109].

The formation of hydroxyl radicals by wavelength λ < 300 nm

$$O_3 + H_2O \xrightarrow{hv} H_2O_2 + O_2$$

$$H_2O_2 \xrightarrow{hv} 2OH^{\cdot}$$

The formation of hydroxyl radicals by wavelength λ > 300 nm

$$O_3 + H_2O \xrightarrow{hv} OH^{\cdot} + HO_2^{\cdot} + O_2$$

2.5.4 Photo-Fenton system

Photo-Fenton system is a combination of Fenton reaction and UV/oxidant system. This system will produce a large amount of active hydroxyl radicals by photo reduction of $Fe(OH)^{2+}$[110]. Under the irradiation of UV light, $Fe(OH)^{2+}$ ions absorb radiation to transfer back into iron ions, thus increasing the oxidation rate [111].

$$Fe(OH)^{2+} + hv \rightarrow Fe^{2+} + \cdot OH$$

$$R(CO_2) - Fe^{3+} + hv \rightarrow R(\cdot CO_2) + Fe^{2+} \rightarrow \cdot R + CO_2$$

In addition, heterogeneous iron species catalysts were developed, such as oxides on various supports like silica, activated carbon. The modification of these materials enlarges the range of reaction pH of the photo-Fenton process.

However, several drawbacks were existed for the running of this process, such as high iron concentration remained [112], complex before treatment process, and catalysts recycling [113]. Thereby, the high running cost, healthy effects on operators, and high operating pressures and temperature are the limitations of wide application of phot-Fenton system in wastewater treatment industry.

2.5.5 Photocatalysis

Photocatalysis is a significant AOP technique for decomposition of organic compounds with a high total organic carbon (TOC) removal at mild operating conditions of temperature and pressure. This technique is relied on the additive catalyst into the wastewater with illumination of UV radiation, which can degrade organic pollutants to carbon dioxide and water by an effective and eco-friendly way. In addition, this technique can be operated at neutral pH and does not form by-product of complex sediment. An efficient photocatalyst is defined as a concordantly combination of chemical and photoelectronic properties, as a result of activations of a semiconductor material. Various types of semiconductor materials, such as TiO_2, ZnO, ZnS, have been developed for photocatalytic oxidation of organic contaminants in the remediation of wastewater [114-116]. The commonly used semiconductors as photocatalysts are listed below in Table 2.5.

Table 2.5 Band gap energy and absorption wavelength of semiconductor photocatalysts.

Semiconductor	Band Gap energy (eV)	Wavelength sensitivity (nm)
TiO_2 (anatase)	3.2	388
TiO_2 (rutile)	3.0	413
ZnO	3.2	388
ZnS	3.6	344
Fe_2O_3	2.3	539
$SrTiO_3$	3.2	388
WO_3	2.8	443

Photocatalytic process is achieved with the absorption of photos by a semiconductor material migrating the electrons from valence band (VB) to conduction band (CB), thereby generating the electron (e^-)/hole (h^+) pairs. The hole (h^+) will react with water and hydroxyl

anions to produce hydroxyl radicals ($OH^{\cdot}$) [117]. The mechanism of the redox reaction can be seen in the following equations [118, 119].

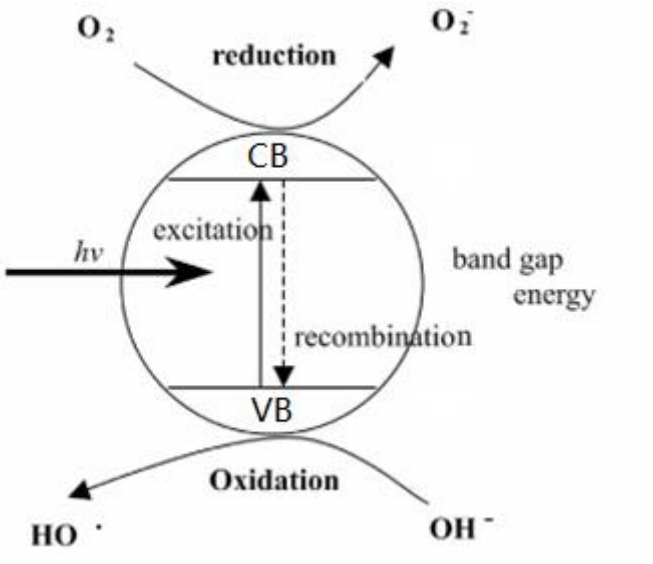

Figure 2.3 Mechanism of photocatalysis process

$$TiO_2 \xrightarrow{hv} e^- + TiO_2(h^+)$$

$$TiO_2(h^+) + H_2O_{ad} \rightarrow TiO_2 + HO^{\cdot}_{ad} + H^+$$

$$TiO_2(h^+) + HO_{ad} \rightarrow TiO_2 + HO^{\cdot}_{ad}$$

$$TiO_2(h^+) + RX_{ad} \rightarrow TiO_2 + RX^{\cdot +}_{ad}$$

Or

$$RX_{ad} + H_2O + O_2 \rightarrow \frac{hv}{TiO_2} \rightarrow H_2O + CO_2 + Mineral.Acid.$$

Generally, the rate of photocatalytic decomposition is affected by illumination intensity, photocatalyst, operating pH, oxygen concentration, and the concentration of organic compounds. Among them, the operating pH value is the most significant factor for photocatalytic reaction, because many properties such as the semiconductor's surface state and the flat-band potential are highly pH dependent. The rate of photocatalytic

decomposition has been modelled by the Langmuir-Hinshelwood (L-H). The Langmuir-Hinshelwood (L-H) kinetics, which is the most commonly used kinetic expression to explain the kinetics of the heterogeneous catalytic processes, can be expressed as follow equation [120].

$$-\frac{dC}{dt} = K_1 K_2 C = kC$$

Among the semiconductors used in photocatalysis, TiO_2 and ZnO have been investigated a lot to be ideal photocatalysts, because of their relatively low price, and excellent photocatalytic performance with maximum quantum yields [116, 121]. In the case of hydrogen peroxide, the generation rate of hydroxyl radicals ($OH^{\cdot}$) could be enhanced by the addition of H_2O_2. Because of the similar properties of ZnO and TiO_2, the applications of TiO_2 are possible to be employed on ZnO photocatalysts. Studies reported that the improvement of decomposition of ampicillin and amoxicillin antibiotics in aqueous solution with TiO_2 photocatalyst under H_2O_2/UV [122]. The combination of PDS or PMS with photocatalysts could also improve the contaminants degradation under the UV irradiation. Some researchers also reported that the addition of $S_2O_8^{2-}$ highly increased the decomposition rate of organic compounds [123-125].

Nevertheless, semiconductors such as ZnO, TiO_2, ZnS that commonly used as photocatalysts exist some disadvantages: large band gap, requiring UV light to achieve electron excitation; instability in aqueous phase; and rapid recombination of photo-generated electron-hole pairs. Thus, photo-stable and effective photocatalysts under visible light are highly required [126, 127]. Heterogeneous photocatalytic oxidation with visible light photocatalysts has attracted a lot of researchers' attention. The photo-generated electrons from the pollutants are transferred to the semiconductors by the absorption of visible light. The mechanism is following the steps as bellow [124].

$$Pollutant + hv \rightarrow Pollutant^{*} \rightarrow Pollutant^{+} + e^{-}$$

$$TiO_2 + e^{-} \rightarrow TiO_2^{\cdot -}$$

$$TiO_2^{\cdot -} + O_2 \rightarrow TiO_2 + O_2^{\cdot -}$$

$$O_2^{\cdot -} + 2H_2O + e^{-} \rightarrow 2H_2O_2$$

$$H_2O_2 + e^- \rightarrow OH^{\cdot} + OH^-$$

A foreign element (Cr, Fe, Mn, Co, etc.) doped into TiO_2 and ZnO as photocatalysts have been investigated for a long time, and most of doped photocatalysts can achieve the photocomposition of organics in aqueous phase with visible light irradiation. Studies showed that metal ion dopants into the TiO_2 can affect the performance of photocatalyst through the dynamics of electrons-holes recombination and interfacial charge transfer [128]. The nanosized TiO_2 particles with the dopants within 1-2 nm of surface have been indicated that the large surface areas make the enhancement of the photocatalytic activity under visible light irradiation [129]. Recent studies [130, 131] reported few heterogeneous Co^{2+} based photocatalysts supported on TiO_2 also can degrade organic pollutants under both UV light and visible light. In addition, inorganic materials such as silica, activated carbon, carbon nanotubes etc. have been employed in extensive investigations of visible light photocatalysts [132-134]. Recently, graphitic carbon nitride (g-C_3N_4), as a marvellous visible light photocatalyst, has attracted a lot of attention.

2.6 Graphitic Carbon Nitride (g-C_3N_4)

Graphitic carbon nitride (g-C_3N_4), a polymeric semiconductor, has recently attracted attention. G-C_3N_4 possesses many advantages such as excellent chemical stability, tunable electronic structure, and medium band gap (2.7eV)[135]. These distinct properties make g-C_3N_4 meet the requirement as a visible light photocatalyst. Moreover, g-C_3N_4 is easily prepared by polymerization of inexpensive feedstocks like cyanamide, urea, melamine and etc. [136-139].

However, pure g-C_3N_4 suffers from several drawbacks: high electron-hole recombination rates, a small specific surface area and low visible light utilization efficiency. Thus, the exploration of facile approaches to synthesize modified g-C_3N_4-based photocatalysts is required to enhance the physicochemical properties and photocatalytic activities. Recently, some strategies have been applied to improve the visible light photocatalytic activity of g-C_3N_4, such as formation of surface coupling hybridization [140], construction of mesoporous structures [141], and doping with metal or non-metal species [142]. Among

these, formation of heterostructures produces the great enhancement of the photocatalytic performance of g-C_3N_4, due to the separation of the electron-hole pairs, and the recombination could be restrained by charge carriers transferring across the interface of the heterostructure. In a coupling process, g-C_3N_4 could combine with visible light excited photocatalysts with a narrow band gap, as well as combine with UV excited semiconductor materials with large band gap, which can extend the application of the g-C_3N_4-based photocatalysts [138, 143]. In addition, the crystal structure of heterostructure can significantly strengthen the quantum efficiency of the photocatalysts.

Recently, g-C_3N_4-based photocatalysts have been employed for photocatalytic decomposition of organic pollutants. For instance, Xu et al. [144] reported that multi-walled carbon nanotubes (CNT) modified C_3N_4 composite (CNT/white C_3N_4) greatly enhance photocatalytic performance in methylene blue (MB) dye removal. The CNT/C_3N_4 composite is also stable enough to have great photocatalytic activity after repeated MB removal experiments. In addition, Zhao et al. [145] reported a WO_3/g-C_3N_4 composite showed a great improvement in photocatalytic degradation of methylene orange under visible light irradiation. In the WO_3/g-C_3N_4 composite, photo-generated electrons and holes can be separated effectively and the recombination rate would be restrained. Furthermore, the composite of g-C_3N_4 and other semiconductor photocatalysts have been reported showing the high photocatalytic performance of decomposition of organic pollutants in wastewater. The composite such as TiO_2/g-C_3N_4, CeO_2/g-C_3N_4, and g-C_3N_4/TaON, exhibits the enhancement in both performance and stability, which are attributed to the effective separation and transfer of photogenerated charges from the well-matched overlapping band-structures and closely contacted interfaces.

2.7 Conclusions

As described above, a huge amount of organic compounds are discharged in wastewater from industrial processes and human activities. These synthetic organic compounds such as polycyclic aromatic hydrocarbons (PAHs), polychlorinated biphenyls (PCBs), di-(2-ethyhexyl)-phthalate (DEHP), benzene, phenols, and dyes, are toxic in aqueous phase, and can cause many human diseases like cancer and genic mutation. A variety of techniques

have been employed to remove these pollutants in wastewater. Wet air oxidation (WAO) and catalytic wet air oxidation (CWAO) are commonly used technologies that are applied in wastewater treatment, however, the commercialization of WAO and CWAO is still a challenge. Advanced oxidation processes (AOPs), which are based on the formation of hydroxyl radical or sulphate radical as an oxidant agent to degrade organic pollutant, are the promising technologies that are effective and can be operated at ambient conditions. Chemical oxidation is a technique using reagents to transform organic compounds in wastewater into harmless components, although many other substances such as minerals which are not the targeted substances may be reacted. Chemical oxidation processes constitute the use of reagents to generate hydroxyl radicals, which oxidize organic compounds in wastewater into harmless components. Nevertheless, the use of individual oxidant to oxidize more complex materials is not efficient because of the low reaction rate. Fenton chemistry is an important technique to degrade organic compounds by using ferrous ions (Fe^{2+}) in aqueous acidic medium, however, the limitations such as requiring acidic condition, a large amount of chemical reagents, and the large production of ferric hydroxide sludge, are required to be settled. Photocatalysis has demonstrated removal of toxic organic pollutants by using semiconductor materials as photocatalysts under the radiation. Due to the continual research, the appropriate radiation wavelength of the modified semiconductor materials has been enlarged from UV light to visible light radiation. In addition, graphitic carbon nitride (g-C_3N_4), an easily-prepared polymeric semiconductor, possesses excellent properties as a photocatalyst. And extensive research indicated the better photocatalytic activity of the modified g-C_3N_4-based photocatalysts in photodegradation of organic pollutant. Thus, photocatalysis processes using modified g-C_3N_4-based photocatalysts are most suitable to degrade organic compounds in aqueous solutions due to low running costs, less energy consumption and high decomposition of organics.

References

1. Robertson, L.W., W. Sulkowski, and B. Hennig, *Preface.* Environmental Toxicology and Pharmacology, 2008. **25**(2): p. 127.

2. Porta, M. and E. Zumeta, *Editorial: Implementing the Stockholm Treaty on Persistent Organic Pollutants.* Occupational and Environmental Medicine, 2002. **59**(10): p. 651-652.

3. Berg, M.V.d., et al., *Toxic Equivalency Factors (TEFs) for PCBs, PCDDs, PCDFs for Humans and Wildlife.* Environmental Health Perspectives, 1998. **106**(12): p. 775-792.

4. Li, R., et al., *Effects of DEHP on endometrial receptivity and embryo implantation in pregnant mice.* Journal of Hazardous Materials, 2012. **241–242**(0): p. 231-240.

5. Silva, M.J., et al., *Urinary levels of seven phthalate metabolites in the U.S. population from the National Health and Nutrition Examination Survey (NHANES) 1999-2000.* Environmental Health Perspectives, 2004. **112**(3): p. 331-338.

6. Takashima, K., et al., *Different Mechanisms of DEHP-induced Hepatocellular Adenoma Tumorigenesis in Wild-type and Pparα-null Mice.* Journal of Occupational Health, 2008. **50**(2): p. 169-180.

7. Miura, Y., et al., *Short-term effects of di-(2-ethylhexyl) phthalate on testes, liver, kidneys and pancreas in mice.* Asian journal of andrology, 2007. **9**(2): p. 199-205.

8. Amorati, R. and L. Valgimigli, *Modulation of the antioxidant activity of phenols by non-covalent interactions.* Organic & Biomolecular Chemistry, 2012. **10**(21): p. 4147-4158.

9. Khoddami, A., M. Wilkes, and T. Roberts, *Techniques for Analysis of Plant Phenolic Compounds.* Molecules, 2013. **18**(2): p. 2328-2375.

10. Silva, P.J., *Inductive and Resonance Effects on the Acidities of Phenol, Enols, and Carbonyl α-Hydrogens.* The Journal of Organic Chemistry, 2008. **74**(2): p. 914-916.

11. Rehfuss, M. and J. Urban, *Rhodococcus phenolicus sp. nov., a novel bioprocessor isolated actinomycete with the ability to degrade chlorobenzene, dichlorobenzene and phenol as sole carbon sources.* Systematic and Applied Microbiology, 2005. **28**(8): p. 695-701.

12. Guillory, J.K., *The Merck Index: An Encyclopedia of Chemicals, Drugs, and Biologicals Edited by Maryadele J. O'Neil, Patricia E. Heckelman, Cherie B. Koch, and Kristin J. Roman. Merck, John Wiley & Sons, Inc., Hoboken, NJ. 2006. xiv + 2564 pp. 18 × 26 cm. ISBN-13 978-0-911910-001. $125.00.* Journal of Medicinal Chemistry, 2006. **50**(3): p. 590-590.

13. Vadivelan, V. and K.V. Kumar, *Equilibrium, kinetics, mechanism, and process design for the sorption of methylene blue onto rice husk.* Journal of Colloid and Interface Science, 2005. **286**(1): p. 90-100.

14. Arami, M., et al., *Removal of dyes from colored textile wastewater by orange peel adsorbent: Equilibrium and kinetic studies.* Journal of Colloid and Interface Science, 2005. **288**(2): p. 371-376.

15. Doğan, M., et al., *Kinetics and mechanism of removal of methylene blue by adsorption onto perlite.* Journal of Hazardous Materials, 2004. **109**(1–3): p. 141-148.

16. Meshko, V., et al., *Adsorption of basic dyes on granular acivated carbon and natural zeolite.* Water Research, 2001. **35**(14): p. 3357-3366.

17. Garg, V.K., et al., *Basic dye (methylene blue) removal from simulated wastewater by adsorption using Indian Rosewood sawdust: a timber industry waste.* Dyes and Pigments, 2004. **63**(3): p. 243-250.

18. Luck, F., *A review of industrial catalytic wet air oxidation processes.* Catalysis Today, 1996. **27**(1–2): p. 195-202.

19. Li, L., P. Chen, and E.F. Gloyna, *Generalized kinetic model for wet oxidation of organic compounds.* AIChE Journal, 1991. **37**(11): p. 1687-1697.

20. Luck, F., *Wet air oxidation: past, present and future.* Catalysis Today, 1999. **53**(1): p. 81-91.

21. Arslan-Alaton, I. and J.L. Ferry, *Application of polyoxotungstates as environmental catalysts: wet air oxidation of acid dye Orange II.* Dyes and Pigments, 2002. **54**(1): p. 25-36.

22. Portela Miguélez, J.R., et al., *Kinetics of wet air oxidation of phenol.* Chemical Engineering Journal, 1997. **67**(2): p. 115-121.

23. Imamura, S., *Catalytic and Noncatalytic Wet Oxidation.* Industrial & Engineering Chemistry Research, 1999. **38**(5): p. 1743-1753.

24. Bhargava, S.K., et al., *Wet Oxidation and Catalytic Wet Oxidation.* Industrial & Engineering Chemistry Research, 2006. **45**(4): p. 1221-1258.

25. Patterson, D.A., et al., *Wet Air Oxidation of Linear Alkylbenzene Sulfonate 2. Effect of pH.* Industrial & Engineering Chemistry Research, 2001. **40**(23): p. 5517-5525.

26. López Bernal, J., et al., *Wet air oxidation of oily wastes generated aboard ships: kinetic modeling.* Journal of Hazardous Materials, 1999. **67**(1): p. 61-73.

27. Willms, R.S., et al., *Aqueous-phase oxidation: the intrinsic kinetics of single organic compounds.* Industrial & Engineering Chemistry Research, 1987. **26**(1): p. 148-154.

28. Laughlin, R.G.W., T. Gallo, and H. Robey, *Wet air oxidation for hazardous waste control.* Journal of Hazardous Materials, 1983. **8**(1): p. 1-9.

29. Bhargava, S., et al., *Catalytic Wet Air Oxidation of Industrial Aqueous Streams.* Catalysis Surveys from Asia, 2007. **11**(1-2): p. 70-86.

30. Zhang, Y., et al., *Catalytic wet air oxidation of dye pollutants by polyoxomolybdate nanotubes under room condition.* Applied Catalysis B: Environmental, 2009. **86**(3–4): p. 182-189.

31. Perathoner, S. and G. Centi, *Wet hydrogen peroxide catalytic oxidation (WHPCO) of organic waste in agro-food and industrial streams.* Topics in Catalysis, 2005. **33**(1-4): p. 207-224.

32. Pirkanniemi, K. and M. Sillanpää, *Heterogeneous water phase catalysis as an environmental application: a review.* Chemosphere, 2002. **48**(10): p. 1047-1060.

33. Gallezot, P., et al., *Catalytic Wet Air Oxidation of Acetic Acid on Carbon-Supported Ruthenium Catalysts.* Journal of Catalysis, 1997. **168**(1): p. 104-109.

34. Imamura, S., A. Doi, and S. Ishida, *Wet oxidation of ammonia catalyzed by cerium-based composite oxides.* Industrial & Engineering Chemistry Product Research and Development, 1985. **24**(1): p. 75-80.

35. Esplugas, S., et al., *Comparison of different advanced oxidation processes for phenol degradation.* Water Research, 2002. **36**(4): p. 1034-1042.

36. Matatov-Meytal, Y.I. and M. Sheintuch, *Catalytic Abatement of Water Pollutants.* Industrial & Engineering Chemistry Research, 1998. **37**(2): p. 309-326.

37. Herrmann, J.-M., *Heterogeneous photocatalysis: fundamentals and applications to the removal of various types of aqueous pollutants.* Catalysis Today, 1999. **53**(1): p. 115-129.

38. Zhang, Q. and K.T. Chuang, *Alumina-Supported Noble Metal Catalysts for Destructive Oxidation of Organic Pollutants in Effluent from a Softwood Kraft Pulp Mill.* Industrial & Engineering Chemistry Research, 1998. **37**(8): p. 3343-3349.

39. Pintar, A., M. Besson, and P. Gallezot, *Catalytic wet air oxidation of Kraft bleach plant effluents in a trickle-bed reactor over a Ru/TiO2 catalyst.* Applied Catalysis B: Environmental, 2001. **31**(4): p. 275-290.

40. Minh, D.P., et al., *Degradation of olive oil mill effluents by catalytic wet air oxidation: 2-Oxidation of p-hydroxyphenylacetic and p-hydroxybenzoic acids over Pt and Ru supported catalysts.* Applied Catalysis B: Environmental, 2007. **73**(3–4): p. 236-246.

41. Barbier, J., Jr., et al., *Role of ceria-supported noble metal catalysts (Ru, Pd, Pt) in wet air oxidation of nitrogen and oxygen containing compounds.* Topics in Catalysis, 2005. **33**(1-4): p. 77-86.

42. Lee, D.-K. and D.-S. Kim, *Catalytic wet air oxidation of carboxylic acids at atmospheric pressure.* Catalysis Today, 2000. **63**(2–4): p. 249-255.

43. Gallezot, P., N. Laurain, and P. Isnard, *Catalytic wet-air oxidation of carboxylic acids on carbon-supported platinum catalysts.* Applied Catalysis B: Environmental, 1996. **9**(1–4): p. L11-L17.

44. Gomes, H.T., J.L. Figueiredo, and J.L. Faria, *Catalytic wet air oxidation of low molecular weight carboxylic acids using a carbon supported platinum catalyst.* Applied Catalysis B: Environmental, 2000. **27**(4): p. L217-L223.

45. Yang, S., M. Besson, and C. Descorme, *Catalytic wet air oxidation of formic acid over Pt/CexZr1−xO2 catalysts at low temperature and atmospheric pressure.* Applied Catalysis B: Environmental, 2010. **100**(1–2): p. 282-288.

46. Barbier Jr, J., et al., *Total oxidation of acetic acid in aqueous solutions over noble metal catalysts.* Journal of Catalysis, 1998. **177**(2): p. 378-385.

47. Roy, S. and A.K. Saroha, *Ceria promoted [gamma]-Al2O3 supported platinum catalyst for catalytic wet air oxidation of oxalic acid: kinetics and catalyst deactivation.* RSC Advances, 2014. **4**(100): p. 56838-56847.

48. Imamura, S., I. Fukuda, and S. Ishida, *Wet oxidation catalyzed by ruthenium supported on cerium(IV) oxides.* Industrial & Engineering Chemistry Research, 1988. **27**(4): p. 718-721.

49. Sadana, A.J., *INVOLVEMENT OF FREE RADICALS IN THE CATALYTIC OXIDATION OF PHENOL IN AQUEOUS SOLUTION*. 1975, University of Delaware: Ann Arbor. p. 205-205 p.

50. Lavelle, K. and J.B. McMonagle, *Mass transfer effects in the oxidation of aqueous organic compounds over a hydrophobic solid catalyst.* Chemical Engineering Science, 2001. **56**(17): p. 5091-5102.

51. Baldi, G., et al., *Catalytic Oxidation of Formic Acid in Water. Intraparticle Diffusion in Liquid-Filled Pores.* Industrial & Engineering Chemistry Process Design and Development, 1974. **13**(4): p. 447-452.

52. Kochetkova, R.P., et al., *Liquid phase catalytic oxidation of phenol.* Chemistry and Technology of Fuels and Oils, 1992. **28**(4): p. 225-229.

53. Kim, K.-H. and S.-K. Ihm, *Heterogeneous catalytic wet air oxidation of refractory organic pollutants in industrial wastewaters: A review.* Journal of Hazardous Materials, 2011. **186**(1): p. 16-34.

54. Sadana, A. and J.R. Katzer, *Involvement of free radicals in the aqueous-phase catalytic oxidation of phenol over copper oxide.* Journal of Catalysis, 1974. **35**(1): p. 140-152.

55. Maurya, M.R. and S. Sikarwar, *Oxidation of phenol and hydroquinone catalysed by copper(II) and oxovanadium(IV) complexes of N,N′-bis(salicyledene)diethylenetriamine (H2saldien) covalently bonded to chloromethylated polystyrene.* Journal of Molecular Catalysis A: Chemical, 2007. **263**(1–2): p. 175-185.

56. Pintar, A. and J. Levec, *Catalytic oxidation of organics in aqueous solutions: I. Kinetics of phenol oxidation.* Journal of Catalysis, 1992. **135**(2): p. 345-357.

57. Pintar, A. and J. Levec, *Catalytic liquid-phase oxidation of refractory organics in waste water.* Chemical Engineering Science, 1992. **47**(9–11): p. 2395-2400.

58. Pintar, A., *Catalytic processes for the purification of drinking water and industrial effluents.* Catalysis Today, 2003. **77**(4): p. 451-465.

59. Levec, J. and A. Pintar, *Catalytic wet-air oxidation processes: A review.* Catalysis Today, 2007. **124**(3–4): p. 172-184.

60. Stüber, F., et al., *Carbon materials and catalytic wet air oxidation of organic pollutants in wastewater.* Topics in Catalysis, 2005. **33**(1-4): p. 3-50.

61. Qin, J., Q. Zhang, and K.T. Chuang, *Catalytic wet oxidation of p-chlorophenol over supported noble metal catalysts.* Applied Catalysis B: Environmental, 2001. **29**(2): p. 115-123.

62. Santos, A., et al., *Route of the catalytic oxidation of phenol in aqueous phase.* Applied Catalysis B: Environmental, 2002. **39**(2): p. 97-113.

63. Santos, A., et al., *Kinetic model of wet oxidation of phenol at basic pH using a copper catalyst.* Chemical Engineering Science, 2005. **60**(17): p. 4866-4878.

64. Santos, A., et al., *Lower toxicity route in catalytic wet oxidation of phenol at basic pH by using bicarbonate media.* Applied Catalysis B: Environmental, 2004. **53**(3): p. 181-194.

65. Fortuny, A., et al., *Water pollution abatement by catalytic wet air oxidation in a trickle bed reactor.* Catalysis Today, 1999. **53**(1): p. 107-114.

66. Fortuny, A., et al., *Catalytic removal of phenol from aqueous phase using oxygen or air as oxidant.* Catalysis Today, 1995. **24**(1–2): p. 79-83.

67. Miró, C., et al., *Aqueous phase catalytic oxidation of phenol in a trickle bed reactor: effect of the pH.* Water Research, 1999. **33**(4): p. 1005-1013.

68. Ohta, H., S. Goto, and H. Teshima, *Liquid-Phase Oxidation of Phenol in a Rotating Catalytic Basket Reactor.* Industrial & Engineering Chemistry Fundamentals, 1980. **19**(2): p. 180-185.

69. Chen, H., et al., *Composition–activity effects of Mn–Ce–O composites on phenol catalytic wet oxidation.* Applied Catalysis B: Environmental, 2001. **32**(3): p. 195-204.

70. Hussain, S.T., A. Sayari, and F.ç. Larachi, *Novel K-Doped Mn–Ce–O Wet Oxidation Catalysts with Enhanced Stability.* Journal of Catalysis, 2001. **201**(1): p. 153-157.

71. Hussain, S.T., A. Sayari, and F.ç. Larachi, *Enhancing the stability of Mn–Ce–O WETOX catalysts using potassium.* Applied Catalysis B: Environmental, 2001. **34**(1): p. 1-9.

72. Levec, J. and A. Pintar, *Catalytic oxidation of aqueous solutions of organics. An effective method for removal of toxic pollutants from waste waters.* Catalysis Today, 1995. **24**(1–2): p. 51-58.

73. Levec, J., M. Herskowitz, and J.M. Smith, *An active catalyst for the oxidation of acetic acid solutions.* AIChE Journal, 1976. **22**(5): p. 919-920.

74. Belkacemi, K., F.ç. Larachi, and A. Sayari, *Lumped Kinetics for Solid-Catalyzed Wet Oxidation: A Versatile Model.* Journal of Catalysis, 2000. **193**(2): p. 224-237.

75. Hamoudi, S., K. Belkacemi, and F.ç. Larachi, *Catalytic oxidation of aqueous phenolic solutions catalyst deactivation and kinetics.* Chemical Engineering Science, 1999. **54**(15–16): p. 3569-3576.

76. Mvndale, V.D., et al., *Regeneration of spent activated carbon by wet air oxidation.* The Canadian Journal of Chemical Engineering, 1991. **69**(5): p. 1149-1159.

77. Nakonechny, M., K. Ikehata, and M. Gamal El-Din, *Kinetics of Estrone Ozone/Hydrogen Peroxide Advanced Oxidation Treatment.* Ozone: Science & Engineering, 2008. **30**(4): p. 249-255.

78. Andreozzi, R., et al., *Advanced oxidation processes (AOP) for water purification and recovery.* Catalysis Today, 1999. **53**(1): p. 51-59.

79. Anipsitakis, G.P. and D.D. Dionysiou, *Radical Generation by the Interaction of Transition Metals with Common Oxidants.* Environmental Science & Technology, 2004. **38**(13): p. 3705-3712.

80. Shukla, P., et al., *Cobalt exchanged zeolites for heterogeneous catalytic oxidation of phenol in the presence of peroxymonosulphate.* Applied Catalysis B: Environmental, 2010. **99**(1–2): p. 163-169.

81. Fu, Y., et al., *Quantum-Chemical Predictions of Absolute Standard Redox Potentials of Diverse Organic Molecules and Free Radicals in Acetonitrile.* Journal of the American Chemical Society, 2005. **127**(19): p. 7227-7234.

82. Gallard, H. and U. von Gunten, *Chlorination of natural organic matter: kinetics of chlorination and of THM formation.* Water Research, 2002. **36**(1): p. 65-74.

83. Waldemer, R.H. and P.G. Tratnyek, *Kinetics of Contaminant Degradation by Permanganate.* Environmental Science & Technology, 2005. **40**(3): p. 1055-1061.

84. Yan, Y.E. and F.W. Schwartz, *Oxidative degradation and kinetics of chlorinated ethylenes by potassium permanganate.* Journal of Contaminant Hydrology, 1999. **37**(3–4): p. 343-365.

85. Huang, K.-C., et al., *Oxidation of chlorinated ethenes by potassium permanganate: a kinetics study.* Journal of Hazardous Materials, 2001. **87**(1–3): p. 155-169.

86. Huang, K.-C., R.A. Couttenye, and G.E. Hoag, *Kinetics of heat-assisted persulfate oxidation of methyl tert-butyl ether (MTBE).* Chemosphere, 2002. **49**(4): p. 413-420.

87. Johnson, R.L., P.G. Tratnyek, and R.O.B. Johnson, *Persulfate Persistence under Thermal Activation Conditions.* Environmental Science & Technology, 2008. **42**(24): p. 9350-9356.

88. Battino, R., T.R. Rettich, and T. Tominaga, *The Solubility of Oxygen and Ozone in Liquids.* Journal of Physical and Chemical Reference Data, 1983. **12**(2): p. 163-178.

89. Quero-Pastor, M., et al., *Degradation of drugs in water with advanced oxidation processes and ozone.* Journal of Environmental Management, 2014. **137**(0): p. 197-203.

90. De Laat, J., G. Truong Le, and B. Legube, *A comparative study of the effects of chloride, sulfate and nitrate ions on the rates of decomposition of H2O2 and organic compounds by Fe(II)/H2O2 and Fe(III)/H2O2.* Chemosphere, 2004. **55**(5): p. 715-723.

91. Walling, C. and A. Goosen, *Mechanism of the ferric ion catalyzed decomposition of hydrogen peroxide. Effect of organic substrates.* Journal of the American Chemical Society, 1973. **95**(9): p. 2987-2991.

92. Pignatello, J.J., E. Oliveros, and A. MacKay, *Advanced Oxidation Processes for Organic Contaminant Destruction Based on the Fenton Reaction and Related Chemistry.* Critical Reviews in Environmental Science and Technology, 2006. **36**(1): p. 1-84.

93. Shimizu, A., et al., *Phenol removal using zero-valent iron powder in the presence of dissolved oxygen: Roles of decomposition by the Fenton reaction and adsorption/precipitation.* Journal of Hazardous Materials, 2012. **201–202**(0): p. 60-67.

94. Zhao, J., et al., *Enhanced oxidation of 4-chlorophenol using sulfate radicals generated from zero-valent iron and peroxydisulfate at ambient temperature.* Separation and Purification Technology, 2010. **71**(3): p. 302-307.

95. Ortiz de la Plata, G.B., O.M. Alfano, and A.E. Cassano, *2-Chlorophenol degradation via photo Fenton reaction employing zero valent iron nanoparticles.* Journal of Photochemistry and Photobiology A: Chemistry, 2012. **233**(0): p. 53-59.

96. Martínez, F., et al., *Influence of preoxidizing treatments on the preparation of iron-containing activated carbons for catalytic wet peroxide oxidation of phenol.* Journal of Chemical Technology & Biotechnology, 2012. **87**(7): p. 880-886.

97. Ramirez, J.H., et al., *Azo-dye Orange II degradation by heterogeneous Fenton-like reaction using carbon-Fe catalysts.* Applied Catalysis B: Environmental, 2007. **75**(3–4): p. 312-323.

98. Duarte, F., et al., *Fenton-like degradation of azo-dye Orange II catalyzed by transition metals on carbon aerogels.* Applied Catalysis B: Environmental, 2009. **85**(3–4): p. 139-147.

99. Ghosh, T., et al., *The characteristic study and sonocatalytic performance of CdSe–graphene as catalyst in the degradation of azo dyes in aqueous solution under dark conditions.* Ultrasonics Sonochemistry, 2013. **20**(2): p. 768-776.

100. Guo, J., et al., *Synthesis of Fe nanoparticles@graphene composites for environmental applications.* Journal of Hazardous Materials, 2012. **225–226**(0): p. 63-73.

101. Zhou, T., et al., *Oxidation of 4-chlorophenol in a heterogeneous zero valent iron/H2O2 Fenton-like system: Kinetic, pathway and effect factors.* Separation and Purification Technology, 2008. **62**(3): p. 551-558.

102. Zhou, T., et al., *Enhanced degradation of 2,4-dichlorophenol by ultrasound in a new Fenton like system (Fe/EDTA) at ambient circumstance.* Ultrasonics Sonochemistry, 2008. **15**(5): p. 782-790.

103. Moon, B.-H., Y.-B. Park, and K.-H. Park, *Fenton oxidation of Orange II by pre-reduction using nanoscale zero-valent iron.* Desalination, 2011. **268**(1–3): p. 249-252.

104. Babuponnusami, A. and K. Muthukumar, *Removal of phenol by heterogenous photo electro Fenton-like process using nano-zero valent iron.* Separation and Purification Technology, 2012. **98**(0): p. 130-135.

105. Benitez, F.J., et al., *Rate constants for the reactions of ozone with chlorophenols in aqueous solutions.* Journal of Hazardous Materials, 2000. **79**(3): p. 271-285.

106. Hirvonen, A., T. Tuhkanen, and P. Kalliokoski, *Formation of chlorinated acetic acids during UV/H2O2-oxidation of ground water contaminated with chlorinated ethylenes.* Chemosphere, 1996. **32**(6): p. 1091-1102.

107. Hirvonen, A., T. Tuhkanen, and P. Kalliokoski, *Treatment of TCE- and PCE contaminated groundwater using UV/H2O2 and O3/H2O2 oxidation processes.* Water Science and Technology, 1996. **33**(6): p. 67-73.

108. De, A.K., S. Bhattacharjee, and B.K. Dutta, *Kinetics of Phenol Photooxidation by Hydrogen Peroxide and Ultraviolet Radiation.* Industrial & Engineering Chemistry Research, 1997. **36**(9): p. 3607-3612.

109. Benitez, F.J., et al., *Simultaneous photodegradation and ozonation plus UV radiation of phenolic acids—major pollutants in agro-industrial wastewaters.* Journal of Chemical Technology & Biotechnology, 1997. **70**(3): p. 253-260.

110. Ting, W.-P., M.-C. Lu, and Y.-H. Huang, *The reactor design and comparison of Fenton, electro-Fenton and photoelectro-Fenton processes for mineralization of benzene sulfonic acid (BSA).* Journal of Hazardous Materials, 2008. **156**(1–3): p. 421-427.

111. Lee, C. and J. Yoon, *Determination of quantum yields for the photolysis of Fe(III)-hydroxo complexes in aqueous solution using a novel kinetic method.* Chemosphere, 2004. **57**(10): p. 1449-1458.

112. Li, D., et al., *Accelerated photobleaching of Orange II on novel (H5FeW12O4010H2O)/silica structured fabrics.* Water Research, 2004. **38**(16): p. 3541-3550.

113. González-Bahamón, L.F., et al., *Photo-Fenton degradation of resorcinol mediated by catalysts based on iron species supported on polymers.* Journal of Photochemistry and Photobiology A: Chemistry, 2011. **217**(1): p. 201-206.

114. Liqiang, J., et al., *Deactivation and regeneration of ZnO and TiO2 nanoparticles in the gas phase photocatalytic oxidation of n-C7H16 or SO2.* Applied Catalysis A: General, 2004. **275**(1–2): p. 49-54.

115. Shang, J., et al., *Comparative Studies on the Deactivation and Regeneration of TiO2 Nanoparticles in Three Photocatalytic Oxidation Systems: C7H16, SO2, and C7H16–SO2.* Journal of Solid State Chemistry, 2002. **166**(2): p. 395-399.

116. Jing, L., et al., *The surface properties and photocatalytic activities of ZnO ultrafine particles.* Applied Surface Science, 2001. **180**(3–4): p. 308-314.

117. Romero, M., et al., *SOLAR PHOTOCATALYTIC DEGRADATION OF WATER AND AIR POLLUTANTS: CHALLENGES AND PERSPECTIVES.* Solar Energy, 1999. **66**(2): p. 169-182.

118. Legrini, O., E. Oliveros, and A.M. Braun, *Photochemical processes for water treatment.* Chemical Reviews, 1993. **93**(2): p. 671-698.

119. Turchi, C.S. and D.F. Ollis, *Photocatalytic degradation of organic water contaminants: Mechanisms involving hydroxyl radical attack.* Journal of Catalysis, 1990. **122**(1): p. 178-192.

120. Kumar, K.V., K. Porkodi, and F. Rocha, *Langmuir–Hinshelwood kinetics – A theoretical study.* Catalysis Communications, 2008. **9**(1): p. 82-84.

121. Chen, H., C.E. Nanayakkara, and V.H. Grassian, *Titanium Dioxide Photocatalysis in Atmospheric Chemistry.* Chemical Reviews, 2012. **112**(11): p. 5919-5948.

122. Elmolla, E.S. and M. Chaudhuri, *Photocatalytic degradation of amoxicillin, ampicillin and cloxacillin antibiotics in aqueous solution using UV/TiO2 and UV/H2O2/TiO2 photocatalysis.* Desalination, 2010. **252**(1–3): p. 46-52.

123. Malato, S., et al., *Optimising solar photocatalytic mineralisation of pesticides by adding inorganic oxidising species; application to the recycling of pesticide containers.* Applied Catalysis B: Environmental, 2000. **28**(3–4): p. 163-174.

124. Konstantinou, I.K. and T.A. Albanis, *TiO2-assisted photocatalytic degradation of azo dyes in aqueous solution: kinetic and mechanistic investigations: A review.* Applied Catalysis B: Environmental, 2004. **49**(1): p. 1-14.

125. Do, S.-H., et al., *Application of a peroxymonosulfate/cobalt (PMS/Co(II)) system to treat diesel-contaminated soil.* Chemosphere, 2009. **77**(8): p. 1127-1131.

126. Comparelli, R., et al., *UV-induced photocatalytic degradation of azo dyes by organic-capped ZnO nanocrystals immobilized onto substrates.* Applied Catalysis B: Environmental, 2005. **60**(1–2): p. 1-11.

127. Serpone, N., et al., *Exploiting the interparticle electron transfer process in the photocatalysed oxidation of phenol, 2-chlorophenol and pentachlorophenol: chemical evidence for electron and hole transfer between coupled semiconductors.* Journal of Photochemistry and Photobiology A: Chemistry, 1995. **85**(3): p. 247-255.

128. Choi, W., A. Termin, and M.R. Hoffmann, *The Role of Metal Ion Dopants in Quantum-Sized TiO2: Correlation between Photoreactivity and Charge Carrier Recombination Dynamics.* The Journal of Physical Chemistry, 1994. **98**(51): p. 13669-13679.

129. Beydoun, D., et al., *Role of Nanoparticles in Photocatalysis.* Journal of Nanoparticle Research, 1999. **1**(4): p. 439-458.

130. Yang, Q., et al., *Heterogeneous activation of peroxymonosulfate by supported cobalt catalysts for the degradation of 2,4-dichlorophenol in water: The effect of support, cobalt precursor, and UV radiation.* Applied Catalysis B: Environmental, 2008. **77**(3–4): p. 300-307.

131. Anipsitakis, G.P., E. Stathatos, and D.D. Dionysiou, *Heterogeneous Activation of Oxone Using Co3O4.* The Journal of Physical Chemistry B, 2005. **109**(27): p. 13052-13055.

132. Saito, T., K. Matsushige, and K. Tanaka, *Chemical treatment and modification of multi-walled carbon nanotubes.* Physica B: Condensed Matter, 2002. **323**(1–4): p. 280-283.

133. Matos, J., J. Laine, and J.M. Herrmann, *Effect of the Type of Activated Carbons on the Photocatalytic Degradation of Aqueous Organic Pollutants by UV-Irradiated Titania.* Journal of Catalysis, 2001. **200**(1): p. 10-20.

134. Herrmann, J.-M., et al., *Solar photocatalytic degradation of 4-chlorophenol using the synergistic effect between titania and activated carbon in aqueous suspension.* Catalysis Today, 1999. **54**(2–3): p. 255-265.

135. Yang, S., et al., *Graphene-Based Carbon Nitride Nanosheets as Efficient Metal-Free Electrocatalysts for Oxygen Reduction Reactions.* Angewandte Chemie International Edition, 2011. **50**(23): p. 5339-5343.

136. Ge, L. and C. Han, *Synthesis of MWNTs/g-C3N4 composite photocatalysts with efficient visible light photocatalytic hydrogen evolution activity.* Applied Catalysis B: Environmental, 2012. **117–118**(0): p. 268-274.

137. Ge, L., et al., *Enhanced visible light photocatalytic activity of novel polymeric g-C3N4 loaded with Ag nanoparticles.* Applied Catalysis A: General, 2011. **409–410**(0): p. 215-222.

138. Liu, W., et al., *Significantly enhanced visible-light photocatalytic activity of g-C3N4 via ZnO modification and the mechanism study.* Journal of Molecular Catalysis A: Chemical, 2013. **368–369**(0): p. 9-15.

139. Yang, Y., et al., *Preparation and enhanced visible-light photocatalytic activity of silver deposited graphitic carbon nitride plasmonic photocatalyst.* Applied Catalysis B: Environmental, 2013. **142–143**(0): p. 828-837.

140. Yan, S.C., et al., *Organic-inorganic composite photocatalyst of g-C3N4 and TaON with improved visible light photocatalytic activities.* Dalton Transactions, 2010. **39**(6): p. 1488-1491.

141. Su, F., et al., *mpg-C3N4-Catalyzed Selective Oxidation of Alcohols Using O2 and Visible Light.* Journal of the American Chemical Society, 2010. **132**(46): p. 16299-16301.

142. Zhang, Y., et al., *Non-covalent doping of graphitic carbon nitride polymer with graphene: controlled electronic structure and enhanced optoelectronic conversion.* Energy & Environmental Science, 2011. **4**(11): p. 4517-4521.

143. Low, J., et al., *Enhanced visible-light photocatalytic activity of plasmonic Ag and graphene co-modified Bi2WO6 nanosheets.* Physical Chemistry Chemical Physics, 2014. **16**(3): p. 1111-1120.

144. Xu, Y., et al., *The CNT modified white C3N4 composite photocatalyst with enhanced visible-light response photoactivity.* Dalton Transactions, 2013. **42**(21): p. 7604-7613.

145. Zhao, J., et al., *Facile synthesis of WO3 nanorods/g-C3N4 composites with enhanced photocatalytic activity.* Ceramics International, (0).

3

Chapter 3: Modification of g-C_3N_4 with metal oxides for degradation of methylene blue and phenol

Abstract

A series of metal-oxide doped graphitic carbon nitride (Fe_2O_3-g-C_3N_4, Fe_3O_4-g-C_3N_4 and MnO_2-g-C_3N_4) photocatalysts were synthesized using a hydrothermal method. The catalytic performances of these materials were evaluated in liquid-phase heterogeneous activation of peroxymonosulfate (PMS) decomposition of phenol and photocatalytic degradation of methylene blue (MB) under UV-vis light irradiation. Their physicochemical properties were characterized by X-ray diffraction (XRD), UV-vis diffusion reflectance spectroscopy, Fourier transform infrared spectroscopy (FTIR), and thermogravimetric analysis (TGA). The experimental results showed that MnO_2-g-C_3N_4 exhibited higher activity than Fe_2O_3-g-C_3N_4 and Fe_3O_4-g-C_3N_4 in photodecomposition of organic compounds in liquid phase. Based on the analysis, we speculated that the physical and optical properties of g-C_3N_4 have been changed upon metal deposition, the enhanced photocatalytic activity of MnO_2-g-C_3N_4 can be attributed to the large heterojunction interface and intrinsically layered structure.

3.1 Introduction

In recent years, graphitic carbon nitride (g-C_3N_4) has received more and more attention due to its unique properties. It was found that g-C_3N_4 has excellent properties such as high thermal and chemical stabilities, and versatile optical, electronic and catalytic properties [1-5]. Graphitic carbon nitride is considered to be a promising candidate for photocatalysis, which makes it valuable material in various potential applications.

The structure of g-C_3N_4 is similar to graphite but not the same. The hexatomic ring consisted of carbon atoms and nitrogen atoms one by one. Every carbon atom has covalent bonds with three nitrogen atoms, thus forming a large planer network structure. As a kind of typical carbon nitride, g-C_3N_4 has been widely used in catalysis. A large amount of researches have been carried out in photodegradation of water pollutants [6, 7], catalysis of organic reactions and carrier for metal catalysts [8, 9].

For water purification, an optical material is needed that has a band gap to absorb visible light, strong oxidative ability and high stability in a complex water solution system [7, 10]. Graphite carbon nitride (g-C_3N_4) has the photocatalytic performance for hydrogen or oxygen production from water splitting under visible light irradiation [6]. Very recently, the g-C_3N_4-metal compounds were found to degrade organic dyes. The functional organic-metal hybrid material exhibited modified electronic properties [4, 9]. Many attempts such as doping with metal have been made to enhance the photocatalytic efficiency of g-C_3N_4. A significant improvement in photocatalytic of g-C_3N_4 was modified by doping the metal Ti [11].

Various efforts have been concentrated on the synthesis of g-C_3N_4 during the past few years. Graphite carbon nitride was mainly produced by heating the carbon-containing and nitrogen-containing precursors [12-15]. The most common compounds used in synthesis include cyanamide, cyanuric chloride, ethylenediamine with carbon tetrachloride and melamine [16-20]. In addition, the material with regular structure can be synthesized by the use of templates [21-24].

In this study, In order to enhance the photocatalytic activities of the g-C_3N_4 photocatalysts, we reported a simple hydrothermal process for synthesis of g-C_3N_4 by pyrolysis approach

and modified by doping Fe_3O_4, Fe_2O_3 and MnO_2. Morphology and structure of the resultant products were characterized by XRD. The photocatalytic activities of the g-C_3N_4 photocatalysts will be evaluated in decomposition of methylene blue in water with UV-vis radiations [8, 25, 26].

3.2 Experimental section

3.2.1 Material and chemicals

Melamine (99%), manganese (II) sulphate monohydrate ($MnSO_4 \bullet H_2O$), ammonium persulfate ($(NH_4)_2S_2O_8$), iron (III) chloride hexahydrate ($FeCl_3 \bullet 6H_2O$), iron (II) chloride tetrahydrate ($FeCl_2 \bullet 4H_2O$) and Oxone® ($2KHSO_5 \bullet 3KHSO_4 \bullet K_2SO_4$, PMS) were obtained from Sigma-Aldrich. Ammonia water (25%) and methanol were purchased from Chem-Supply. Phenol was purchased from Ajax Finechem. All the chemicals were used as received without further purification.

3.2.2 Catalyst preparation

3.2.2.1 Synthesis of graphitic carbon nitrides

Graphitic carbon nitrides (g-C_3N_4) were synthesized in a semi-close system [27]. Typically, 10 g melamine were dissolved in 20 mL methanol with continual stirring until mixture became pasty, and then dried in an oven at 50 ℃ overnight. The dried mixture was heated at 550 ℃ in a muffle furnace for 2 hours with a ramp rate of 5 ℃/min. The yellow solid products were grinded into powders for further synthesis.

3.2.2.2 Synthesis of metal oxide-doped graphitic carbon nitrides.

The modified g-C_3N_4 samples were synthesized by a hydrothermal method. In a typical synthesis of Fe_2O_3-g-C_3N_4, 0.36 g $FeCl_2 \bullet 4H_2O$ was dissolved in 50 mL deionized water, and then 2 g of g-C_3N_4 powder were added into the solution. The suspension was transferred into a 100 mL Teflon-lined stainless steel autoclave. The autoclave was put into an oven and heated at 180 ℃ for 18 hours, then cooled down to room temperature. For Fe_3O_4-g-C_3N_4,

0.25g $FeCl_2 \bullet 4H_2O$, 0.70g $FeCl_3 \bullet 6H_2O$ and 2mL ammonia water (25%) were added into 50mL deionized water in an autoclave, and nitrogen gas flow for 10min, then sealed and heated at 180 ℃ for 18 hours, and then cooled down to room temperature naturally. For MnO_2-g-C_3N_4, 0.58g $MnSO_4 \bullet H_2O$ and 0.78g $(NH_4)_2S_2O_8$ were put into an autoclave with 50 mL deionized water, and heated at 140 ℃ for 12 hours, cooled down to room temperature. The resultant precipitate was filtrated, and washed with ethanol and deionized water, then dried in an oven at 60 ℃ for 24 hours. The final products were collected as Mn_2-g-C_3N_4.

3.2.3 Characterization of materials

The crystalline structures and phases of the samples were evaluated by X-ray diffraction (XRD) on a Bruker D8 Advance X-ray instrument using Cu Kα radiation with λ at 1.5418 Å. Fourier transform infrared spectra (FTIR) were obtained on a Perkin-Elmer Model FTIR-100 with a MIR detector. UV-vis diffuse reflectance spectra (DRS) of prepared catalysts were recorded on a UV-vis spectrophotometer (JASCO V670), with $BaSO_4$ as reference standard. Thermogravimetric-differential thermal analysis (TG-DTA) was operated on a Perkin- Elmer Diamond thermal analyser under air flow at a heating rate of 10 ℃/min.

3.2.4 Measurements of catalytic activity

3.2.4.1 The photocatalytic activities test

The photocatalytic activities of the prepared catalysts were carried out by the photocatalytic degradation of dye, methylene blue (MB), in an aqueous solution under visible light irradiation. A 575 W metal halide lamp (Philips) was used as a light source. In detail, 100 mg catalysts were added into 200 mL of 10 mg/L MB solution in a double-jacket cylindrical reactor. The light source was set about 30 cm from the liquid surface of the suspension. The suspension was firstly continual stirring in the dark for 30 min to ensure the dye on the catalyst has reached an adsorption-desorption equilibrium. Then the reaction was started by exposing to visible-light irradiation under continual stirring. During the process, at given time intervals, approximate 5 mL of suspension was collected and centrifuged, and then analysed by a JASCO UV-vis spectrophotometer at 664 nm.

3.2.4.2 Phenol degradation test

Phenol degradation test was evaluated in a 500 mL conical flask with 20 mg/L phenol solution, 0.1 g/L catalyst and 2 g/L oxone®(PMS, widely used as an oxidizing agent) at 25 ℃ with a constant stirring. At given time intervals, 1 mL water sample was withdrawn and filtered (0.45μm) into a vial, and then 0.5 mL of methanol was added into the vial to quench the reaction. The water sample was analysed by a Varian HPLC with a C-18 column.

3.3 Results and discussion

3.3.1 Materials characterization

The XRD patterns of g-C_3N_4 and X- g-C_3N_4 (X= Fe_3O_4, Fe_2O_3 , MnO_2) samples are shown in Figure 3.1. Two peaks can be found in the pattern of g-C_3N_4, the small-angle peak (100) at 13.11° is corresponding to a distance of 0.67 nm [6, 28]. The strongest peak (002) at 2θ=27.42° is a characteristic interlayer stacking peak for graphitic C_3N_4 material. For Fe_3O_4-g-C_3N_4 and Fe_2O_3-g-C_3N_4, the peak (002) moves to 27.99° and 28.02°, respectively. Meanwhile, the peak (002) of MnO_2-g-C_3N_4 is staying at 27.42°.

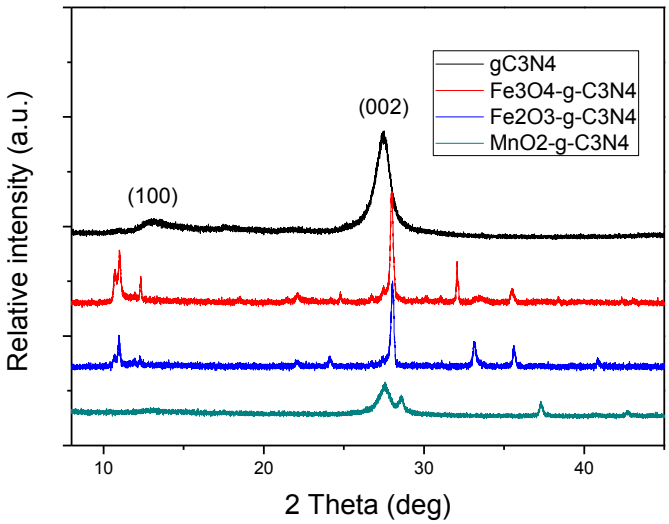

Figure 3.1 XRD patterns of g-C_3N_4 and X-g-C_3N_4

Figure 3.2 shows the diffuse reflectance spectra of g-C_3N_4, Fe_3O_4-g-C_3N_4, Fe_2O_3-g-C_3N_4 and MnO_2-g-C_3N_4. The adsorption edge of g-C_3N_4 was at 470 nm, which is corresponding to the band gap at 2.63 eV [8]. Meanwhile, the adsorption edge of modified g-C_3N_4 exhibited strong light absorption and red shift of adsorption edge [29, 30]. Red shift of adsorption indicated that ease of photoinduced electrons and holes producing.

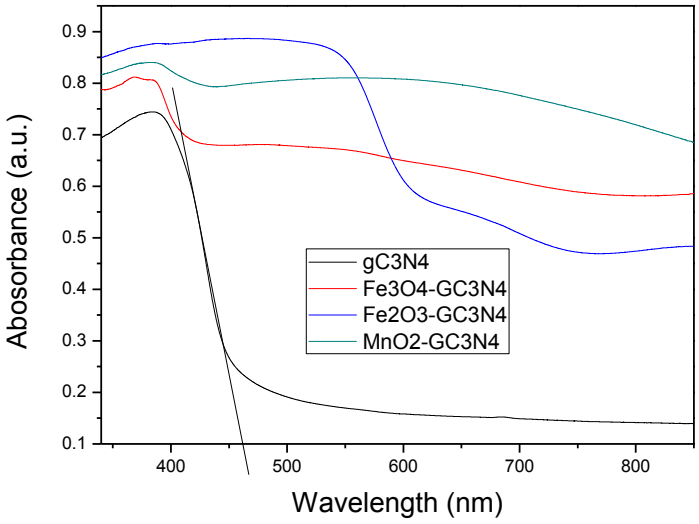

Figure 3.2 UV-vis diffuses reflectance spectra of g-C_3N_4 and X-g-C_3N_4.

The thermal stability of g-C_3N_4 and X-g-C_3N_4 were analysed by thermogravimetric-differential thermal analysis shown in Figure 3.3. A weight loss at the temperature 20-200 ℃ was observed, contributed to the removal of water. Fe_3O_4-g-C_3N_4 and Fe_2O_3-g-C_3N_4 becomes unstable when the heating temperature is over 300 ℃, due to desorption and the decomposition of the functional groups in g-C_3N_4 [31]. The quick weight loss of g-C_3N_4 after 500 ℃ can be ascribed to the combustion of the carbon skeleton and the liberation of oxygen-containing groups. The elemental loading on Fe_2O_3-g-C_3N_4, Fe_3O_4-g-C_3N_4 and MnO_2-g-C_3N_4 were determined based on their TGA profiles to be 22.5%, 12.8% and 11.6%, respectively.

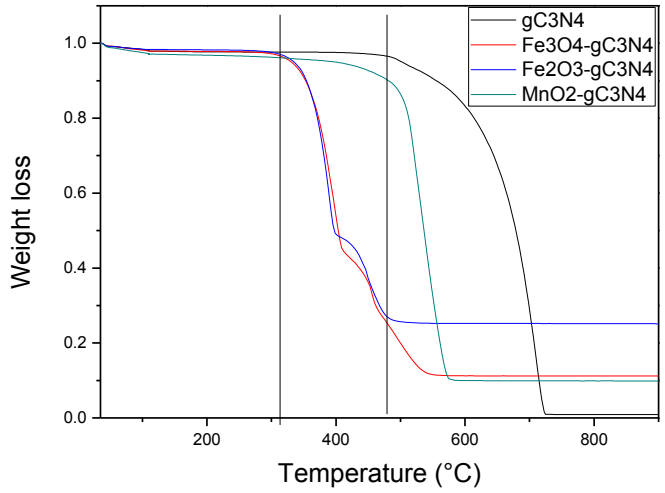

Figure 3.3 TG thermogram curves of g-C_3N_4 and X-g-C_3N_4.

Figure 3.4 shows Fourier transform infrared spectroscopy (FT-IR) spectra of g-C_3N_4 and the modified g-C_3N_4 samples. For g-C_3N_4 samples, peaks at 1030 and 1160 cm^{-1} are attributed to C-O stretching and C-OH stretching, respectively, which indicated the presence of hydroxyl (C-OH), carbonyl (C=O) and carboxylic (COOH). The broad peak at 3100-3300 cm^{-1} [29], is indexed to the N-H stretching or the H_2O adsorption [7, 8]. The characteristic peaks of g-C_3N_4, is corresponding to the typical stretching modes of CN heterocycles between 1240 and 1650 cm^{-1}.

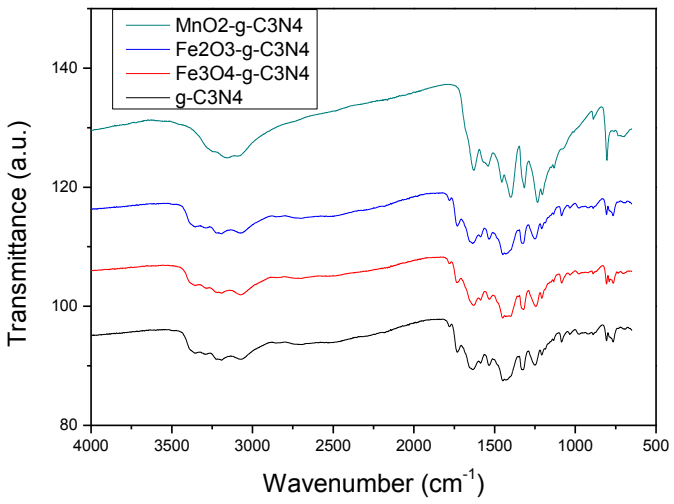

Figure 3.4 FTIR spectra for the g-C_3N_4, Fe_3O_4-g-C_3N_4, Fe_2O_3-g-C_3N_4 and MnO_2-g-C_3N_4.

3.3.2 Catalytic performance

The photocatalytic activities of various g-C_3N_4 were evaluated in degradation of methylene blue (MB) solution under visible light irradiation in Figure 3.5. Under the UV-vis light, the pure g-C_3N_4 can degrade 79% of MB in 180min. In comparison, MnO_2-g-C_3N_4 had a better photocatalytic activity performance that 86% of MB was degraded in 3 hours. Meanwhile, Fe_3O_4-g-C_3N_4 has a similar rate with pure g-C_3N_4 in MB decomposition. By contrast, Fe_2O_3-g-C_3N_4 had a worst performance, only 56% MB was decomposed in 180 min. Generally, modification of g-C_3N_4 with MnO_2 can enhance the photocatalytic activity by degrading MB under irradiation. The g-C_3N_4 doped MnO_2 sample could decompose 86% MB in 3 hours due to the strong adsorption of modified structure toward aromatic structure of MB.

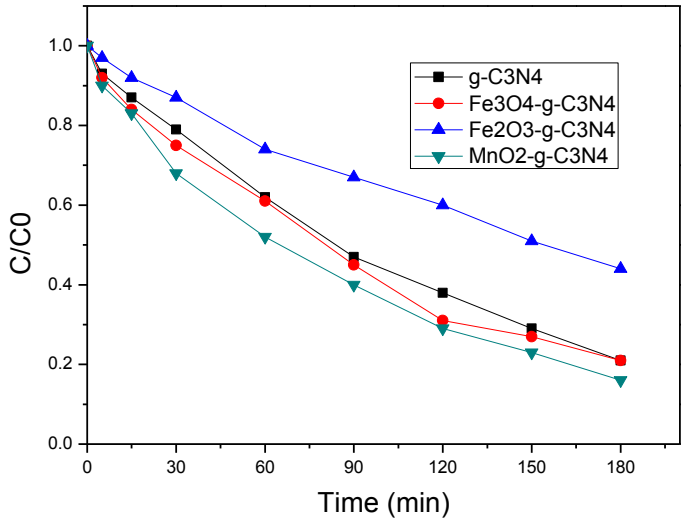

Figure 3.5 Photodegradation of methylene blue solution under UV-vis light.

Figure 3.6 shows the efficiencies of g-C_3N_4 samples in catalytic oxidation of phenol solutions by activation of oxone. Generally, the pure g-C_3N_4 can hardly generate phenol degradation and only approximate 6% phenol was decomposed in 180 min. Meanwhile, the phenol could be oxidized at 36.5% by adding MnO_2-g-C_3N_4, and about 15% phenol can be degraded by adding Fe_3O_4-g-C_3N_4 and Fe_2O_3-g-C_3N_4 as solid catalysts.

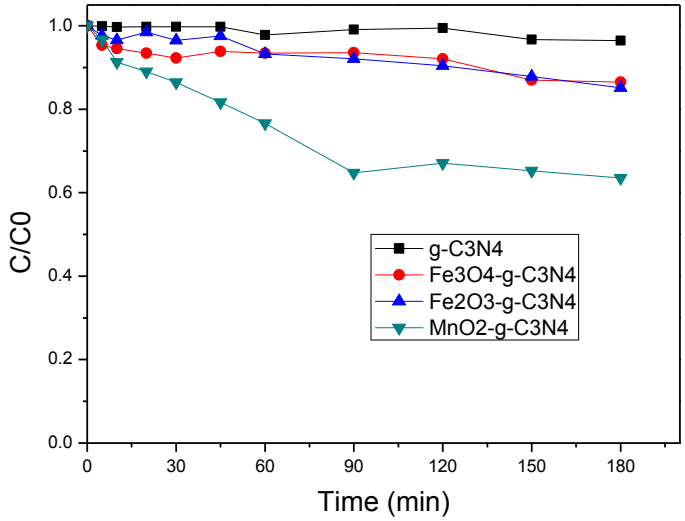

Figure 3.6 Phenol degradation under various g-C_3N_4 samples.

3.4 Conclusions

Metal oxides modified g-C_3N_4 photocatalysts were synthesized by using a hydrothermal method in this study. MnO_2-g-C_3N_4 possessed a better photocatalytic performance in degradation of MB under UV-vis light irradiations and the catalytic oxidation of phenol solution. Introduction of the manganese ions into g-C_3N_4 would improve the structure the catalytic performance of g-C_3N_4.

References

1. Bai, X., C. Cao, and X. Xu, *Formation and characterization of flower-like carbon nitride by pyrolysis of melamine.* Materials Science and Engineering: B, 2010. **175**(2): p. 95-99.

2. Jiang, G., et al., *Controllable preparation of graphitic carbon nitride nanosheets via confined interlayer nanospace of layered clays.* Materials Letters, 2010. **64**(24): p. 2718-2721.

3. Wang, Y., X. Wang, and M. Antonietti, *Polymeric Graphitic Carbon Nitride as a Heterogeneous Organocatalyst: From Photochemistry to Multipurpose Catalysis to Sustainable Chemistry.* Angewandte Chemie International Edition, 2012. **51**(1): p. 68-89.

4. Zhang, J., et al., *Graphitic carbon nitride materials synthesized via reactive pyrolysis routes and their properties.* Diamond and Related Materials, 2011. **20**(3): p. 385-388.

5. Zheng, Y., et al., *Graphitic carbon nitride materials: controllable synthesis and applications in fuel cells and photocatalysis.* Energy & Environmental Science, 2012. **5**(5): p. 6717-6731.

6. Yan, S.C., Z.S. Li, and Z.G. Zou, *Photodegradation of Rhodamine B and Methyl Orange over Boron-Doped g-C3N4 under Visible Light Irradiation.* Langmuir, 2010. **26**(6): p. 3894-3901.

7. Yan, S.C., Z.S. Li, and Z.G. Zou, *Photodegradation Performance of g-C3N4 Fabricated by Directly Heating Melamine.* Langmuir, 2009. **25**(17): p. 10397-10401.

8. Zheng, Y., et al., *Nanoporous Graphitic-C3N4@Carbon Metal-Free Electrocatalysts for Highly Efficient Oxygen Reduction.* Journal of the American Chemical Society, 2011. **133**(50): p. 20116-20119.

9. Wang, X., S. Blechert, and M. Antonietti, *Polymeric Graphitic Carbon Nitride for Heterogeneous Photocatalysis.* ACS Catalysis, 2012. **2**(8): p. 1596-1606.

10. Sun, H., et al., *Supported cobalt catalysts by one-pot aqueous combustion synthesis for catalytic phenol degradation.* Journal of Colloid and Interface Science, 2013. **394**(0): p. 394-400.

11. Chen, L., et al., *Preparation of graphite-like carbon nitride nanoflake film with strong fluorescent and electrochemiluminescent activity.* Nanoscale, 2013. **5**(1): p. 225-230.

12. Zhu, J., et al., *Graphitic carbon nitride as a metal-free catalyst for NO decomposition.* Chemical Communications, 2010. **46**(37): p. 6965-6967.

13. Thomas, A., et al., *Graphitic carbon nitride materials: variation of structure and morphology and their use as metal-free catalysts.* Journal of Materials Chemistry, 2008. **18**(41): p. 4893-4908.

14. Yao, Y., et al., *Magnetic CoFe2O4–Graphene Hybrids: Facile Synthesis, Characterization, and Catalytic Properties.* Industrial & Engineering Chemistry Research, 2012. **51**(17): p. 6044-6051.

15. Cui, Y., et al., *Metal-free activation of H2O2 by g-C3N4 under visible light irradiation for the degradation of organic pollutants.* Physical Chemistry Chemical Physics, 2012. **14**(4): p. 1455-1462.

16. Yang, S., et al., *Graphene-Based Carbon Nitride Nanosheets as Efficient Metal-Free Electrocatalysts for Oxygen Reduction Reactions.* Angewandte Chemie International Edition, 2011. **50**(23): p. 5339-5343.

17. Ge, L. and C. Han, *Synthesis of MWNTs/g-C3N4 composite photocatalysts with efficient visible light photocatalytic hydrogen evolution activity.* Applied Catalysis B: Environmental, 2012. **117–118**(0): p. 268-274.

18. Ge, L., et al., *Enhanced visible light photocatalytic activity of novel polymeric g-C3N4 loaded with Ag nanoparticles.* Applied Catalysis A: General, 2011. **409–410**(0): p. 215-222.

19. Yang, Y., et al., *Preparation and enhanced visible-light photocatalytic activity of silver deposited graphitic carbon nitride plasmonic photocatalyst.* Applied Catalysis B: Environmental, 2013. **142–143**(0): p. 828-837.

20. Zhang, Y., et al., *Non-covalent doping of graphitic carbon nitride polymer with graphene: controlled electronic structure and enhanced optoelectronic conversion.* Energy & Environmental Science, 2011. **4**(11): p. 4517-4521.

21. Su , D.S., et al., *Metal-Free Heterogeneous Catalysis for Sustainable Chemistry.* ChemSusChem, 2010. **3**(2): p. 169-180.

22. Cui, Y., et al., *Metal-free photocatalytic degradation of 4-chlorophenol in water by mesoporous carbon nitride semiconductors.* Catalysis Science & Technology, 2012. **2**(7): p. 1396-1402.

23. Jürgens, B., et al., *Melem (2,5,8-Triamino-tri-s-triazine), an Important Intermediate during Condensation of Melamine Rings to Graphitic Carbon Nitride: Synthesis, Structure Determination by X-ray Powder Diffractometry, Solid-State NMR, and Theoretical Studies.* Journal of the American Chemical Society, 2003. **125**(34): p. 10288-10300.

24. Yan, H., Y. Chen, and S. Xu, *Synthesis of graphitic carbon nitride by directly heating sulfuric acid treated melamine for enhanced photocatalytic H2 production from water under visible light.* International Journal of Hydrogen Energy, 2012. **37**(1): p. 125-133.

25. Shi, R., et al., *Visible-Light Photocatalytic Degradation of BiTaO4 Photocatalyst and Mechanism of Photocorrosion Suppression.* The Journal of Physical Chemistry C, 2010. **114**(14): p. 6472-6477.

26. Ullah, R., et al., *Wet-Chemical Synthesis of InTaO4 for Photocatalytic Decomposition of Organic Contaminants in Air and Water with UV–vis Light.* Industrial & Engineering Chemistry Research, 2011. **51**(4): p. 1563-1569.

27. Xu, J., Y. Wang, and Y. Zhu, *Nanoporous Graphitic Carbon Nitride with Enhanced Photocatalytic Performance.* Langmuir, 2013. **29**(33): p. 10566-10572.

28. Li, X.-H., et al., *Metal-Free Activation of Dioxygen by Graphene/g-C3N4 Nanocomposites: Functional Dyads for Selective Oxidation of Saturated Hydrocarbons.* Journal of the American Chemical Society, 2011. **133**(21): p. 8074-8077.

29. Chang, F., et al., *A facile modification of g-C3N4 with enhanced photocatalytic activity for degradation of methylene blue.* Applied Surface Science, 2013. **280**(0): p. 967-974.

30. Yuan, Y.-P., et al., *Red phosphor/g-C3N4 heterojunction with enhanced photocatalytic activities for solar fuels production.* Applied Catalysis B: Environmental, 2013. **140–141**(0): p. 164-168.

31. Liu, J., et al., *Simple solvothermal synthesis of hydrophobic magnetic monodispersed Fe3O4 nanoparticles.* Materials Research Bulletin, 2013. **48**(2): p. 416-421.

4

Chapter 4: Polyometalate modified graphitic carbon nitride materials for photocatalysis

Abstract

Polyometalate nanoparticles (POMs) and their functionalized graphitic carbon nitride (g-C_3N_4) were synthesized using a facile hydrothermal method. The photocatalysts were characterized by field emission scanning electron microscopy (FESEM), X-ray diffraction (XRD), N_2 sorption isotherms, thermogravimetric analysis (TGA), and UV-vis diffusion reflectance spectroscopy. The photocatalytic properties were investigated in photodecomposition of methylene blue and phenol under UV-visible light irradiations. It was found that the surface area and pore volume have been improved after POMs deposition and that the photocatalysts have enhanced photocatalytic activities. For g-C_3N_4, 80% of methylene blue was removed at 180 min, while it only needs 60 min to achieve by using PMo_{12}@g-C_3N_4-6%, and it can achieve 100% conversion in 180 min. In addition, phenol removal has been enhanced to 52% and 38% by using PMo_{12}@g-C_3N_4-6% and PW_{12}@g-C_3N_4-6% as photocatalysts.

4.1 Introduction

As an undesirable consequence of high-speed urbanization and industrialization, organic pollutants such as phenolics, dyes and pharmaceuticals, discharged from industries and households have become a serious issue to the environment. Due to the strong toxicity of the various organic compounds, effective remediation technologies for removal of the organic pollutants from wastewater are highly demanded.

Generally, advanced oxidation processes (AOPs) are widely employed for complete decomposition of organics into carbon dioxide and water [1, 2]. Among various AOPs, heterogeneous photocatalysis has been considered as a promising remediation technique due to its low-cost, environmental friendliness and sustainability [3]. In heterogeneous photocatalytic reaction, this process is achieved with the absorption of photos by a semiconductor material [4]. The electron (e^-)/hole (h^+) pairs will be generated in the conduction band (CB) and valence band (VB), and migrate the electrons to the surface of semiconductor where redox reactions occur [5-9].

Graphitic carbon nitride (g-C_3N_4) has drawn plenty of interest in the research interest due to its structure and remarkable chemical and physical properties, such as excellent electronic conductivity and great mechanical strength [10]. G-C_3N_4 has great potential in solar energy conversion and storage, photocatalysis and electrocatalysis, photovoltaic devices and bioimaging application [10-13]. Polyoxometalates (POMs) are one of the widely used photoelectrocatalysts in homogeneous and heterogeneous processes [14]. POMs are a vast class of well-defined, early transition metal-oxygen clusters with an enormous diversity of structural characteristics and multiple functions, which have been significantly improving the development of materials with catalytic and photochemical properties [15]. For example, some reports have described a significant improvement in the electrochemical properties of POM/MCN hybrids [16], which offers potentially high activity and selectivity in water oxidation catalysis at the heterogeneous surface of a functional electrode.

Herein, we employed a facile hydrothermal method to synthesize POMs@g-C_3N_4 hybrids. Their physicochemical properties, such as crystalline structure, morphology and thermal stability were investigated. Furthermore, the photocatalytic degradation of methylene blue and phenol were tested.

4.2 Experimental section

4.2.1 Material and chemicals

Melamine (99.0%), phosphomolybdic acid hydrate ($PMo_{12}O_{40}•xH_2O$, >99.0%) and phosphotungstic acid hydrate ($PW_{12}O_{40}•xH_2O$, >99.0%) were obtained for Sigma-Aldrich. Methanol was purchased from Chem-Supply. Phenol (99.0%) was purchased from Ajax Finechem. All the chemicals were used as received without further purification.

4.2.2 Synthesis of polyoxometalate @g-C_3N_4 (POMs@g-C_3N_4)

The synthesis of POMs@g-C_3N_4 hybrids was accomplished by a modified hydrothermal method. In a typical synthesis, 0.408 g of $PMo_{12}O_{40}•xH_2O$ was dissolved in 40 mL deionized water, and then 2 g of g-C_3N_4 powder, which were synthesized by melamine in a semi-close system[17], were added into the aqueous solution. The suspension was transferred into a 100 mL Teflon-lined stainless steel autoclave, and then put in an oven pre-set at 180 ℃ for 12 h. After cooling down to room temperature, the precipitate was collected from the autoclave and washed 3 times with a large amount of deionized water to remove any impurities. The washed product was dried in an oven at 60 ℃ overnight and labelled as PMo_{12}@g-C_3N_4 -2%. The different molecular ratio of PMo_{12}@g-C_3N_4 were synthesised in the same way, and final precipitates were labelled as PMo_{12}@g-C_3N_4-4%, PMo_{12}@g-C_3N_4-6%, PMo_{12}@g-C_3N_4-8%, and PMo12@g-C_3N_4-10%.

The PW_{12}@g-C_3N_4 hybrids were synthesised in the same modified hydrothermal method, above using $PW_{12}O_{40}•xH_2O$ in the molar ratios of 2%, 4%, 6%, 8% and 10%.

4.2.3 Characterization

The crystalline structures and phases of the material was evaluated with X-ray diffraction (XRD) patterns obtained on a Bruker D8 diffractometer (Bruker-AXS, Karlsruhe, Germany) using filtered Cu Kα radiation with λ at 1.5418 Å. Scanning electron microscopy (SEM, Zeiss Neon 40EsB FIBSEM) was performed to obtain the structure and morphology of the materials. The Brunauer-Emmett-Teller (BET) specific surface area and pore size distribution of the samples were conducted by N_2 adsorption/desorption using a Micrometrics Tristar 3000 with the BET and Barrett-Joyner-Halenda (BJH) methods, respectively. UV-vis diffuse

reflectance spectra (DRS) of prepared catalysts were recorded on a UV-vis spectrophotometer (JASCO V670) with an Ø 60 mm integrating sphere and $BaSO_4$ as a reference standard. Thermal stability and phase transformation of POMs@g-C_3N_4 were studied by thermogravimetric-differential thermal analysis (TG-DTA) on a Perkin-Elmer Diamond thermal analyzer under air flow at a heating rate of 10 ℃/min.

4.2.4 Photocatalytic activity and adsorption tests

4.2.4.1 Photocatalytic degradation of methylene blue

Photocatalytic oxidation using POMs@g-C_3N_4 was carried out by the photocatalytic degradation of a dye, methylene blue (MB), under ultraviolet and visible light irradiations. The irradiation source was supplied by a MSR 575/2 metal halide lamp (575 W, Philips). The average intensities of the lamp were measured to be 60 and 84 $\mu W/cm^2$ at 315-400 and 400-1050nm, respectively. In detail, 200 mL MB solution at 10 ppm with 100 mg catalyst were continuously stirred in a 1000 mL double-jacket cylindrical Pyrex vessel reactor. The light source was set about 30 cm from the liquid surface of the suspension. The reaction was started by exposing the UV-vis irradiation after 30 min stirred in dark for achieving the adsorption-desorption equilibrium. The reaction temperature was controlled by recycling the cooling water at 30 ℃ in a water bath. During the process, at given time intervals, approximate 5 mL of suspension were collected and centrifuged, and then analyzed by a JASCO UV-vis spectrophotometer at 664 nm. The degradation efficiency (%) can be calculated as:

$$efficiency(\%) = \frac{C_0 - C}{Co} \times 100\%$$

Where C_0 is the initial concentration of methylene blue, and C is the concentration considering methylene blue degradation on photocatalyst.

4.2.4.2 Photocatalytic degradation of phenol

The photocatalytic degradation of phenol tests were carried out in the similar system with 20 ppm phenol solution. During the process, 1 mL solution was withdraw by a syringe and

filtered by a 0.25 μm Millipore film into a HPLC vial. Then the concentration of phenol was examined on a 380-LC HPLC with a UV detector set at λ = 270 nm.

4.2.4.3 Adsorption test

The adsorption test was run in the same system as photocatalytic reaction without any irradiation.

4.3 Results and discussion

4.3.1 Characterization

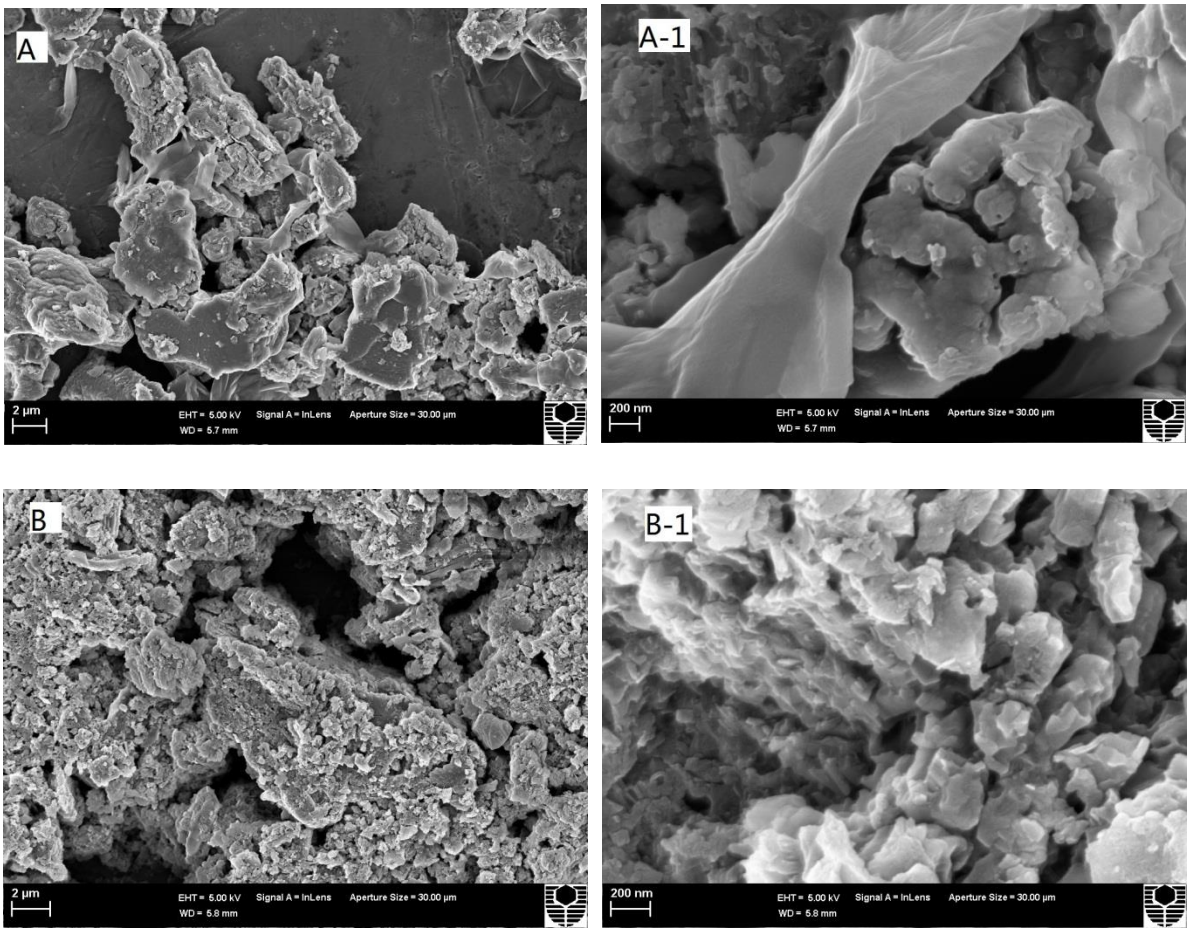

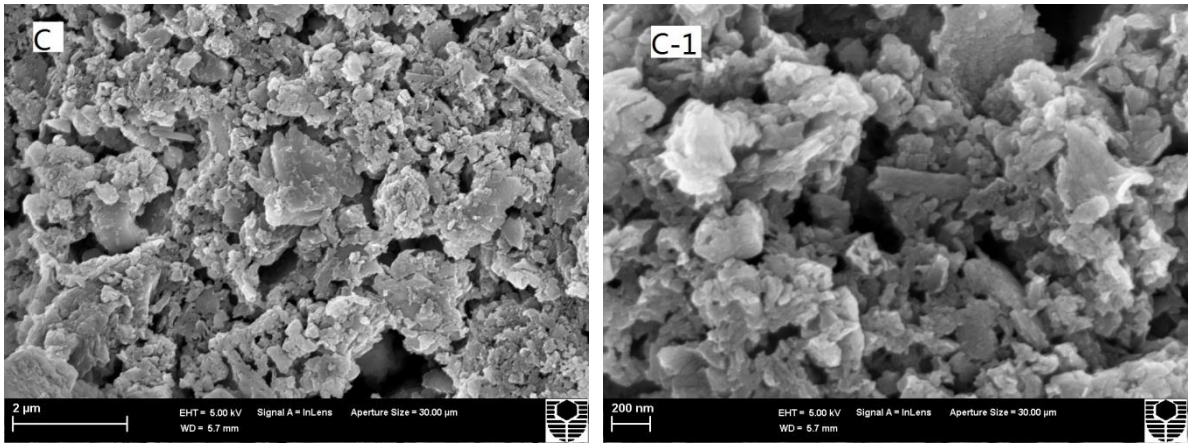

Figure 4.1 SEM images of pure g-C_3N_4 (A, A-1), PMo_{12}@g-C_3N_4 (B, B-1) and PW_{12}@g-C_3N_4(C, C-1).

Morphology and structure of the synthesized materials were investigated by SEM images. Figure 4.1 (A) shows clear, crisp edges and rodlike structures of g-C_3N_4. A high magnification of g-C_3N_4 can be seen in Figure 4.1 (A-1), which shows the nanorods at a size of 5-6 µm in length. As seen, the PMo_{12} and PW_{12} [18] were observed in Figure 4.1(B, B-1, C and C-1), in the hydrothermal condition of mild temperature (180℃) and 12 hours, the morphology of g-C_3N_4 was modified, and parts of laminated structure of g-C_3N_4 were transformed to a smaller rodlike structures.

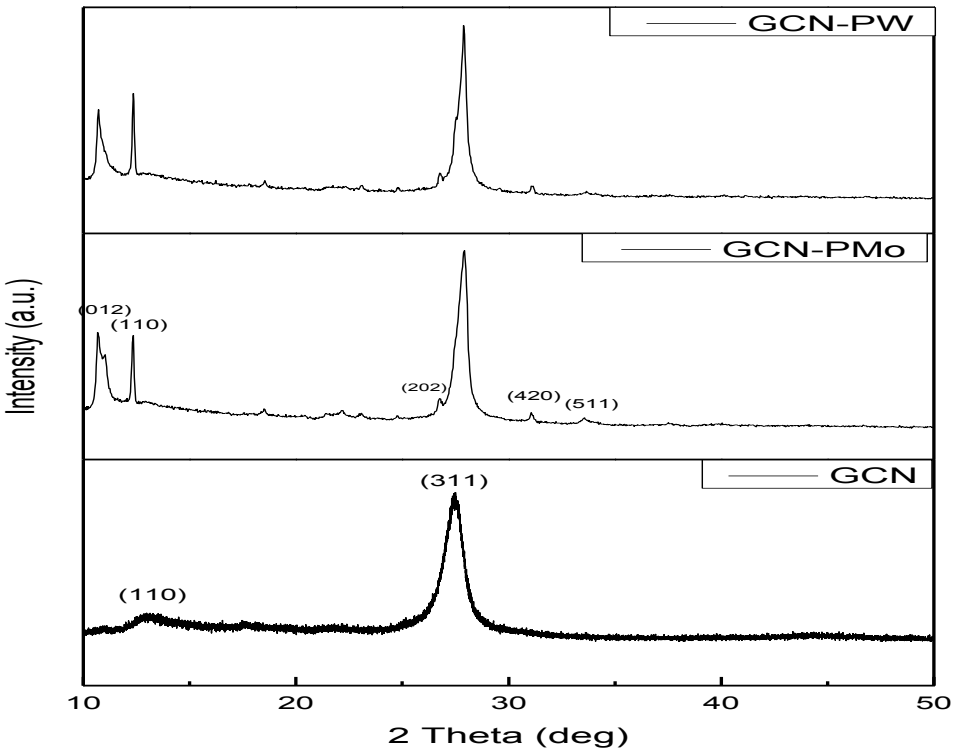

Figure 4.2 XRD patterns of g-C_3N_4 and POMs@g-C_3N_4 samples.

The crystalline structures of prepared g-C_3N_4 and POMs@g-C_3N_4 materials were analyzed by XRD, as shown in Figure 4.2. Same characteristic peaks at 14.1° and 27.4° were observed on g-C_3N_4, PMo_{12}@g-C_3N_4 and PW_{12}@g-C_3N_4. The intensities of the peaks on PMo_{12}@g-C_3N_4 and PW_{12}@g-C_3N_4 were much stronger than those of pure g-C_3N_4. In the patterns of PMo_{12}@g-C_3N_4 and PW_{12}@g-C_3N_4, besides the peaks of g-C_3N_4, peaks at 11.8°, 32.6° and 35.1°, corresponding to characteristic peaks of crystal planes (012), (420) and (511) of POMs, respectively [19]. Another weak peak at 26.4° was possibly due to the (202) face of PO_3 [20].

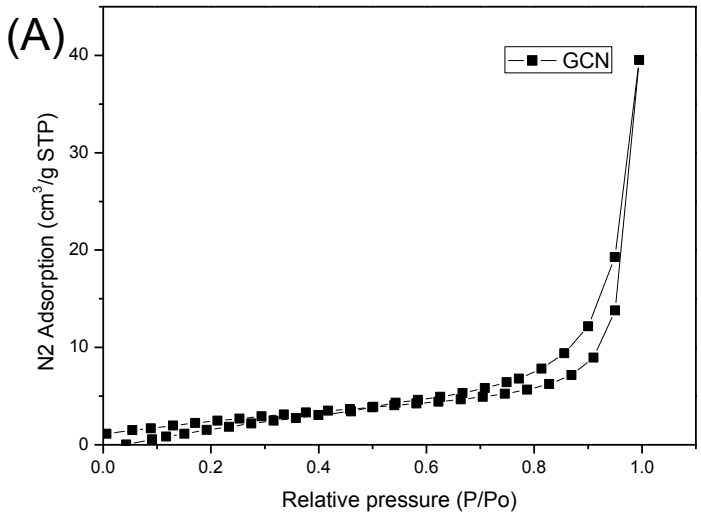
(A)
GCN
N2 Adsorption (cm3/g STP)
Relative pressure (P/Po)
0
10
20
30
40
0.0
0.2
0.4
0.6
0.8
1.0

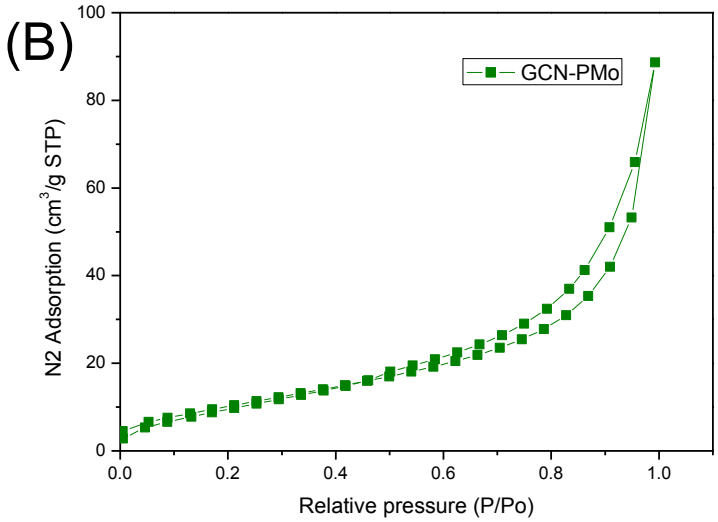
(B)
GCN-PMo
N2 Adsorption (cm3/g STP)
Relative pressure (P/Po)
0
20
40
60
80
100
0.0
0.2
0.4
0.6
0.8
1.0

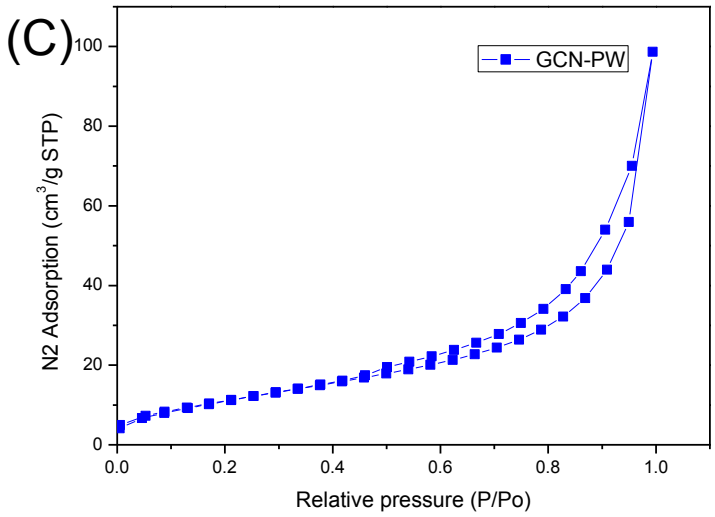

Figure 4.3 N_2 sorption isotherms of three photocatalysts.

Table 4.1 Textural properties of g-C_3N_4 and POMs@g-C_3N_4 samples.

Catalyst	Surface area (S_{BET}, m^2/g)	Pore volume (cm^3/g)	Average pore size (nm)
g-C_3N_4	10.1	0.065	24.1
PW_{12}@g-C_3N_4	33.0	0.136	16.6
PMo_{12}@g-C_3N_4	36.2	0.152	16.8

Figure 4.3 demonstrates N_2 adsorption/desorption isotherms and Table 4.1 shows the surface area, pore volume and pore size of three photocatalysts. In general, all the three samples had an IV isotherm with a type of H3 hysteresis loop, suggesting a mesoporous structure [18]. As seen, PMo_{12}@g-C_3N_4-6% possessed a higher surface area (36.2 m^2/g), which is more than 3 times of that of g-C_3N_4, and the pore volume (0.152 cm^3/g) is also higher. The hysteresis loops at a relative pressure (P/P_0) range of 0.4-0.95 indicated the mesoporous structure of the g-C_3N_4 and POMs@g-C_3N_4 samples.

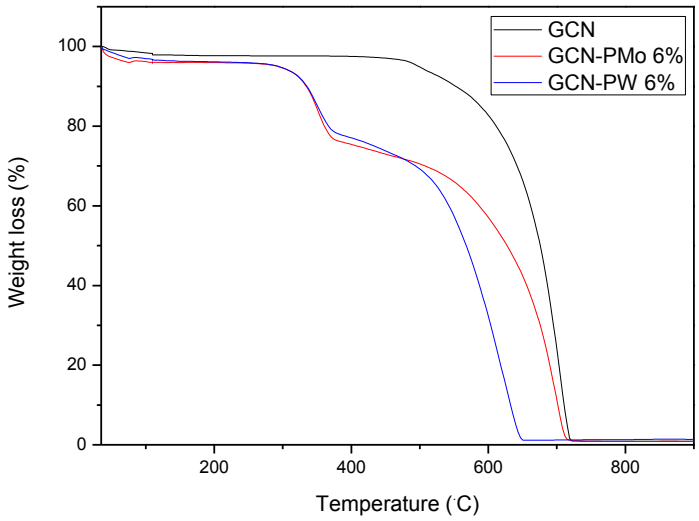

Figure 4.4 TGA curves of photocatalysts.

Figure 4.4 displays TGA profiles of g-C_3N_4 and modified g-C_3N_4 photocatalysts in air atmosphere with a heating rate of 10 ℃/min. As seen, the mild weight loss occurs from 110 to 200 ℃, only adsorbed water or ethanol was removed, and then three endothermic peaks were observed at 305, 378 and 482 ℃, respectively. The PMo_{12} and PW_{12} become unstable when temperature is at 300 - 375 ℃ [21]. The second endothermic peak at 378 ℃ was attributed to the decomposition and combustion of organics and amorphous carbon [19]. After 482 ℃, the carbon nitride was combusted and oxidized into CO_2 and NO_2 at 720 ℃.

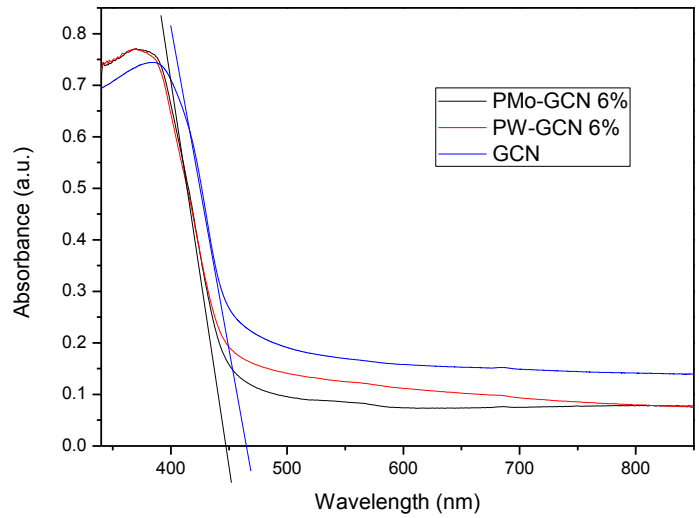

Figure 4.5 Diffuse reflectance spectroscopy of g-C_3N_4 and POMs@g-C_3N_4 samples.

The UV-vis absorption spectra for g-C_3N_4, PMo_{12}@g-C_3N_4-6% and PW_{12}@g-C_3N_4 -6% are shown in Figure 4.5. The PMo_{12} and PW_{12} display absorption across the visible light region ascribed to the d-d transition. The g-C_3N_4 exhibits absorption in the visible light absorption edge at 470 nm, which is corresponding to the band gap at 2.63 eV. Meanwhile, PMo_{12}@g-C_3N_4-6% and PW_{12}@g-C_3N_4 -6% are corresponding to the band gap at 2.75 eV [21-23].

4.3.2 Photocatalytic activity tests

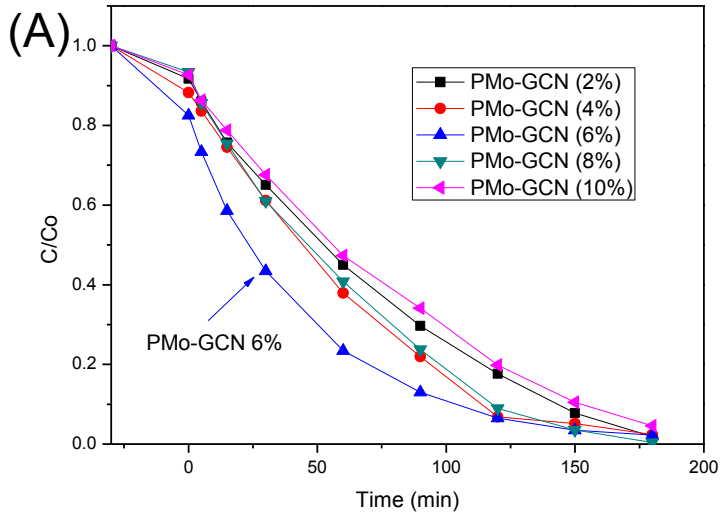

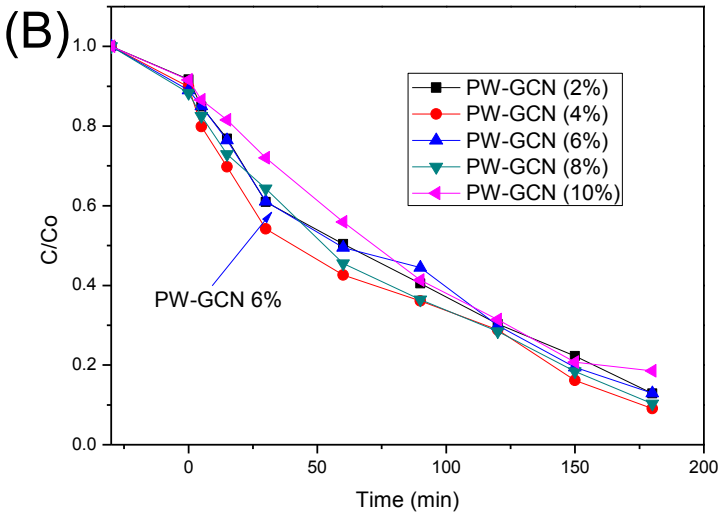

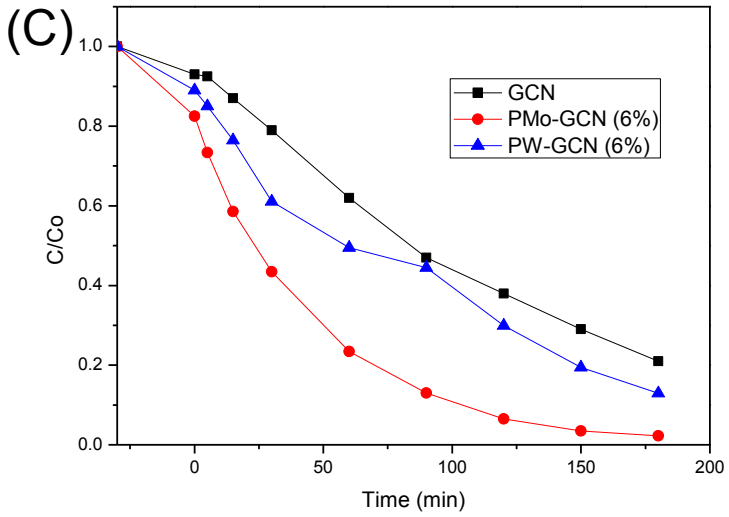

Figure 4.6 Photocatalytic of methylene blue of various PMo_{12}@g-C_3N_4 (A) and PW_{12}@g-C_3N_4 (B) and pure g-C_3N_4 (C) photocatalysts under UV-vis light irradiation.

In Figure 4.6, the effects of various ratios of POMs@g-C_3N_4 in methylene blue degradation under UV-vis light irradiation was showed. It can be seen from Figure (A), all methylene blue can be degraded at 180 min under UV-vis light irradiation by using PMo_{12}@g-C_3N_4 photocatalysts, while various PW_{12}@g-C_3N_4 at different ratios (B) had similar photocatalytic activities that 90 % of methylene blue was removed in 180 min. Pure g-C_3N_4 (C) was used as a reference sample, and 80% of methylene blue was decomposition in 3 hours under irradiation. PMo_{12}@g-C_3N_4-6% produced a higher activity that 80% of methylene blue was removed in 60 min, and it can remove all of methylene blue at 180 min.

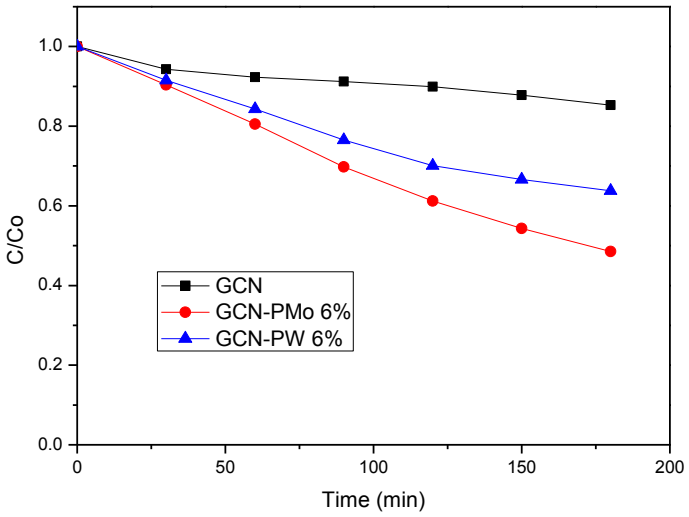

Figure 4.7 Activities of phenol decomposition with photocatalysts.

Figure 4.7 shows that PMo_{12}@g-C_3N_4 -6%, and PW_{12}@g-C_3N_4 -6% had a higher activity than pure g-C_3N_4. Generally, the pure g-C_3N_4 was hardly to make decomposition of phenol, only performing 10% in 180 min, while 6% phenol was being adsorbed by the photocatalyst (Shown below in Figure 4.8). Meanwhile, phenol could be removed at about 52% and 38% by using PMo_{12}@g-C_3N_4 -6%, and PW_{12}@g-C_3N_4 -6% as photocatalysts under 3 hours UV-vis irradiation.

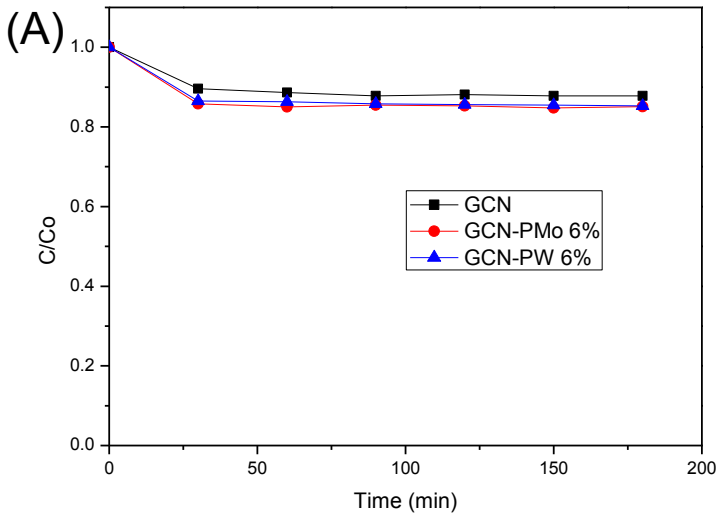

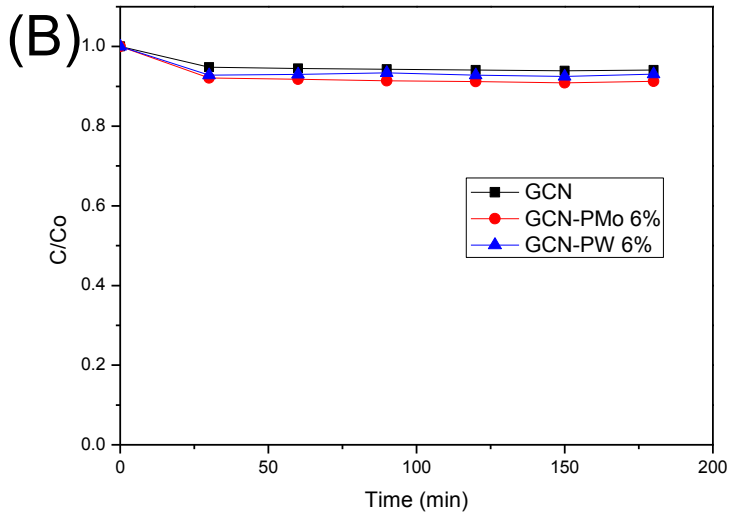

Figure 4.8 Adsorption of MB (A) and phenol (B) on photocatalysts in 3 hours.

Figure 4.8 shows the adsorption of methylene blue and phenol on the pure g-C_3N_4 and POMs@g-C_3N_4 photocatalysts. The results demonstrated that the samples, g-C_3N_4, PMo_{12}@g-C_3N_4 -6%, and PW_{12}@g-C_3N_4 -6%, presented a minor adsorption of methylene blue at 13%, 19% and 15%; and the adsorption of phenol at 6%, 9% and 8%, respectively at 180 min. Thus, the major decreases of methylene blue and phenol concentrations in the catalytic tests were contributed to the photodecomposition of g-C_3N_4 and modified POMs@g-C_3N_4 photocatalysts.

4.4 Conclusion

PMo_{12} and PW_{12} modified g-C_3N_4 photocatalysts were synthesized via a one-step hydrothermal method with varying POMs loading levels. PMo_{12}@g-C_3N_4-6% possessed a higher surface area and pore volume, and showed a better photocatalytic performance in degradation of MB and phenol under UV–vis light irradiations. The modified structure and the matched band structures between POMs and g-C_3N_4 contribute to the enhanced photocatalysis. This study suggested promising material hybrids for photodegradation of aqueous organic pollutants for water remediation.

References

1. Pera-Titus, M., et al., *Degradation of chlorophenols by means of advanced oxidation processes: a general review.* Applied Catalysis B: Environmental, 2004. **47**(4): p. 219-256.

2. Esplugas, S., et al., *Comparison of different advanced oxidation processes for phenol degradation.* Water Research, 2002. **36**(4): p. 1034-1042.

3. Fujishima, A., X. Zhang, and D.A. Tryk, *TiO2 photocatalysis and related surface phenomena.* Surface Science Reports, 2008. **63**(12): p. 515-582.

4. Simonsen, M.E., et al., *Photocatalytic bleaching of p-nitrosodimethylaniline and a comparison to the performance of other AOP technologies.* Journal of Photochemistry and Photobiology A: Chemistry, 2010. **216**(2–3): p. 244-249.

5. Adewuyi, Y.G., *Sonochemistry in Environmental Remediation. 1. Combinative and Hybrid Sonophotochemical Oxidation Processes for the Treatment of Pollutants in Water.* Environmental Science & Technology, 2005. **39**(10): p. 3409-3420.

6. Adewuyi, Y.G., *Sonochemistry in Environmental Remediation. 2. Heterogeneous Sonophotocatalytic Oxidation Processes for the Treatment of Pollutants in Water.* Environmental Science & Technology, 2005. **39**(22): p. 8557-8570.
7. Ji, Y., et al., *Photocatalytic degradation of atenolol in aqueous titanium dioxide suspensions: Kinetics, intermediates and degradation pathways.* Journal of Photochemistry and Photobiology A: Chemistry, 2013. **254**(0): p. 35-44.

8. Mills, A. and S. Le Hunte, *An overview of semiconductor photocatalysis.* Journal of Photochemistry and Photobiology A: Chemistry, 1997. **108**(1): p. 1-35.

9. Carp, O., C.L. Huisman, and A. Reller, *Photoinduced reactivity of titanium dioxide.* Progress in Solid State Chemistry, 2004. **32**(1–2): p. 33-177.

10. Maeda, K., et al., *Photocatalytic Activities of Graphitic Carbon Nitride Powder for Water Reduction and Oxidation under Visible Light.* The Journal of Physical Chemistry C, 2009. **113**(12): p. 4940-4947.

11. Goettmann, F., et al., *Metal-free catalysis of sustainable Friedel-Crafts reactions: direct activation of benzene by carbon nitrides to avoid the use of metal chlorides and halogenated compounds.* Chemical Communications, 2006(43): p. 4530-4532.

12. Zhang, J., et al., *Co-Monomer Control of Carbon Nitride Semiconductors to Optimize Hydrogen Evolution with Visible Light.* Angewandte Chemie International Edition, 2012. **51**(13): p. 3183-3187.

13. Zhang, X., et al., *Enhanced Photoresponsive Ultrathin Graphitic-Phase C3N4 Nanosheets for Bioimaging.* Journal of the American Chemical Society, 2012. **135**(1): p. 18-21.

14. Guo, Y. and C. Hu, *Heterogeneous photocatalysis by solid polyoxometalates.* Journal of Molecular Catalysis A: Chemical, 2007. **262**(1–2): p. 136-148.

15. Okuhara, T., *Microporous heteropoly compounds and their shape selective catalysis.* Applied Catalysis A: General, 2003. **256**(1–2): p. 213-224.

16. Wu, J., et al., *Polyoxometalates Immobilized in Ordered Mesoporous Carbon Nitride as Highly Efficient Water Oxidation Catalysts.* ChemSusChem, 2012. **5**(7): p. 1207-1212.

17. Xu, J., Y. Wang, and Y. Zhu, *Nanoporous Graphitic Carbon Nitride with Enhanced Photocatalytic Performance.* Langmuir, 2013. **29**(33): p. 10566-10572.

18. Suarez-Guevara, J., V. Ruiz, and P. Gomez-Romero, *Stable graphene-polyoxometalate nanomaterials for application in hybrid supercapacitors.* Physical Chemistry Chemical Physics, 2014. **16**(38): p. 20411-20414.

19. Zhou, D. and B.-H. Han, *Graphene-Based Nanoporous Materials Assembled by Mediation of Polyoxometalate Nanoparticles.* Advanced Functional Materials, 2010. **20**(16): p. 2717-2722.

20. Li, H., et al., *Polyoxometalate assisted photoreduction of graphene oxide and its nanocomposite formation.* Chemical Communications, 2010. **46**(34): p. 6243-6245.

21. Wang, S., et al., *Electrochemical-Reduction-Assisted Assembly of a Polyoxometalate/Graphene Nanocomposite and Its Enhanced Lithium-Storage Performance.* Chemistry – A European Journal, 2013. **19**(33): p. 10895-10902.

22. Rodriguez-Albelo, L.M., et al., *[varepsilon]-Keggin-based coordination networks: Synthesis, structure and application toward green synthesis of polyoxometalate@graphene hybrids.* Dalton Transactions, 2012. **41**(33): p. 9989-9999.

23. Liu, R., et al., *A general green strategy for fabricating metal nanoparticles/polyoxometalate/graphene tri-component nanohybrids: enhanced electrocatalytic properties.* Journal of Materials Chemistry, 2012. **22**(8): p. 3319-3322.

5

Chapter 5: Silver Silicate modified graphitic carbon nitride catalysts for photodegradation of methylene blue under UV-vis light irradiations

Abstract

Silver silicate modified graphitic carbon nitride catalysts (g-C_3N_4/$Ag_6Si_2O_7$ composites) were synthesized using a facile hydrolysis and ion-exchange method. The catalysts were tested for removal of methylene blue via photocatalytic decomposition and adsorption. The photocatalytic properties were investigated in liquid-phase degradation of methylene blue under UV-vis light. The characterization of the photocatalysts was conducted by field emission scanning electron microscopy (FESEM), X-ray diffraction (XRD), and UV-vis diffusion reflectance spectroscopy. Compared with g-C_3N_4, the g-C_3N_4/$Ag_6Si_2O_7$ composites showed an enhanced photocatalytic activity in decomposition of methylene blue under UV-vis light irradiations.

5.1 Introduction

In the 21st century, wastewater treatment for its recycling is a significant issue in our lives, because the hazardous components in wastewater have posed great threats to the public health and the shortage of fresh water occurs worldwide[1, 2]. Industrial processes have generated a large amount of organic compounds and discharged into the environment [3, 4]. These organic pollutants, such as phenol and dyes, are toxic and recalcitrant to natural degradation. Therefore, it is urgent to develop effective techniques for removal of the organic contaminants from water.

Advanced oxidation processes (AOPs) have been widely investigated and employed as a viable strategy to degrade organic compounds in wastewater into simple compounds, carbon dioxide and water. Most AOPs are based on the generation of reactive species, such as superoxide radicals ($O_2^{-}\cdot$) and hydroxyl radicals (·OH) that have a high standard oxidation potential for non-selective reaction [5, 6]. Currently, photocatalytic abatement of organic pollutants has drawn plenty of interest from both academic and industrial societies. The photocatalytic reaction is achieved by the excitation of electrons from the valence band (VB) to the conduction band (CB) of semiconductor materials upon irradiation, and the excited electron (e^-)/hole (h^+) pairs can be used in a redox reaction. Thus, photocatalysis is considered as a promising technique for eliminating organic compounds in wastewater via a redox mechanism [7-9].

Graphitic carbon nitride (g-C_3N_4) has been considered as one of the most eminent candidates due to its low toxicity, high stability and appealing electronic structure [10-12]. Nevertheless, the photocatalytic activity is limited by its low surface area and quantum efficiency [13]. Many potential modifications of g-C_3N_4 have been carried out in activity improving.

Silicates have been widely employed as industrial catalysts [14]. A silicate-based photocatalyst [15] has been reported recently owing to desirable photocatalytic activity. $Ag_6Si_2O_7$ has an internal polar electric field by controlling the array of the polar SiO_4 tetrahedra, which coordinate Ag^+ ions leading to AgO_x. $Ag_6Si_2O_7$ exhibits a very high potential in photocatalytic application due to its response in whole visible-light region (λ < 740 nm).

In this study, g-C_3N_4/$Ag_6Si_2O_7$ composites would be synthesized. These composites were tested in photocatalytic degradation of methylene blue under UV-vis light. Furthermore, their physicochemical properties, such as crystalline structure and morphology were observed.

5.2 Experimental section

5.2.1 Material and chemicals

Melamine (99.0%), sodium metasilicate nonahydrate (Na_2SiO_3•$9H_2O$, >99.0%), and silver nitrate ($AgNO_3$, >99.0%) were obtained for Sigma-Aldrich. Methanol was purchased from Chem-Supply. All the chemicals were used without further purification.

5.2.2 Synthesis of g-C_3N_4/$Ag_6Si_2O_7$ composites

Synthesis of $Ag_6Si_2O_7$: In detail, 0.852g Na_2SiO_3•$9H_2O$ was dissolved in 210 ml deionized water under continual stirring. Then the mixture was added gently into 90 ml 0.1M $AgNO_3$ solution to generate reddish brown precipitates. After 30 min stirring, the precipitates were harvested from the solution by vacuum filtration and washed with deionized water for 3 times before drying at 55 ℃ overnight.

Synthesis of g-C_3N_4/$Ag_6Si_2O_7$: 0.284g Na_2SiO_3•$9H_2O$ was dissolved with the 70ml deionized water under continual stirring, then 3.672 g of prepared g-C_3N_4 were added into the solution under ultrasonic treatment for 60 min. The mixture was added gently into 30ml 0.1M $AgNO_3$ solution to generate orange precipitates. After 30 min stirring, the precipitates were harvested from the solution by vacuum filtration and washed with deionized water for 3 times before drying at 55 ℃ overnight. Several g-C_3N_4/$Ag_6Si_2O_7$ at different ratios were synthesised in the same way, and final precipitates were labelled as g-C_3N_4/$Ag_6Si_2O_7$-20%, g-C_3N_4/$Ag_6Si_2O_7$-30%, g-C_3N_4/$Ag_6Si_2O_7$-40%, and g-C_3N_4/$Ag_6Si_2O_7$-50%.

5.2.3 Characterization

X-ray diffraction (XRD) patterns were obtained on a Bruker D8 diffractometer (Bruker-AXS, Karlsruhe, Germany) using filtered Cu Kα radiation with λ at 1.5418 Å. The structure and

morphology of the materials were performed on a scanning electron microscopy (SEM, Zeiss Neon 40EsB FIBSEM). Fourier transform infrared spectra (FT-IR) were acquired from a Perkin-Elmer Model FTIR-100 with a MIR detector. UV-vis diffuse reflectance spectra (DRS) of prepared catalysts were recorded on a JASCO V670 UV-vis spectrophotometer with an Ø 60 mm integrating sphere, in which $BaSO_4$ was used as a reference standard.

5.2.4 Photocatalytic oxidation of methylene blue

The aqueous photocatalytic oxidation of methylene blue was carried out in a 1000 mL double-jacket cylindrical Pyrex vessel reactor. A water bath connected with a pump was used to control the reaction temperature at 30℃ by recycling the cooling water. The light source was set about 30 cm from the liquid surface of the suspension. The irradiation source was supplied by a MSR 575/2 metal halide lamp (575 W, Philips). The UV intensity at 315 -400 was measured to 60 $\mu W/cm^2$ and the visible light intensity at 400 - 1050 nm was 84 $\mu W/cm^2$. In detail, 0.1g of photocatalyst was added into 200 mL of 10 ppm methylene blue solution and stirred 30 min to achieve the adsorption-desorption equilibrium. The light was immediately switched on, and then reaction was started by exposing the UV-vis irradiation. During the process, 3 mL of solution was collected and centrifuged at each time interval, and then analysed by a JASCO UV-vis spectrophotometer at 664 nm. The degradation efficiency (%) can be calculated as:

$$efficiency(\%) = \frac{C_0 - C}{Co} \times 100\%$$

Where C_0 is the initial concentration of methylene blue, and C is the concentration considering methylene blue degradation on a photocatalyst.

The adsorption test was run in the same system as photocatalytic reaction without any irradiation.

5.3 Results and discussion

5.3.1 Characterization

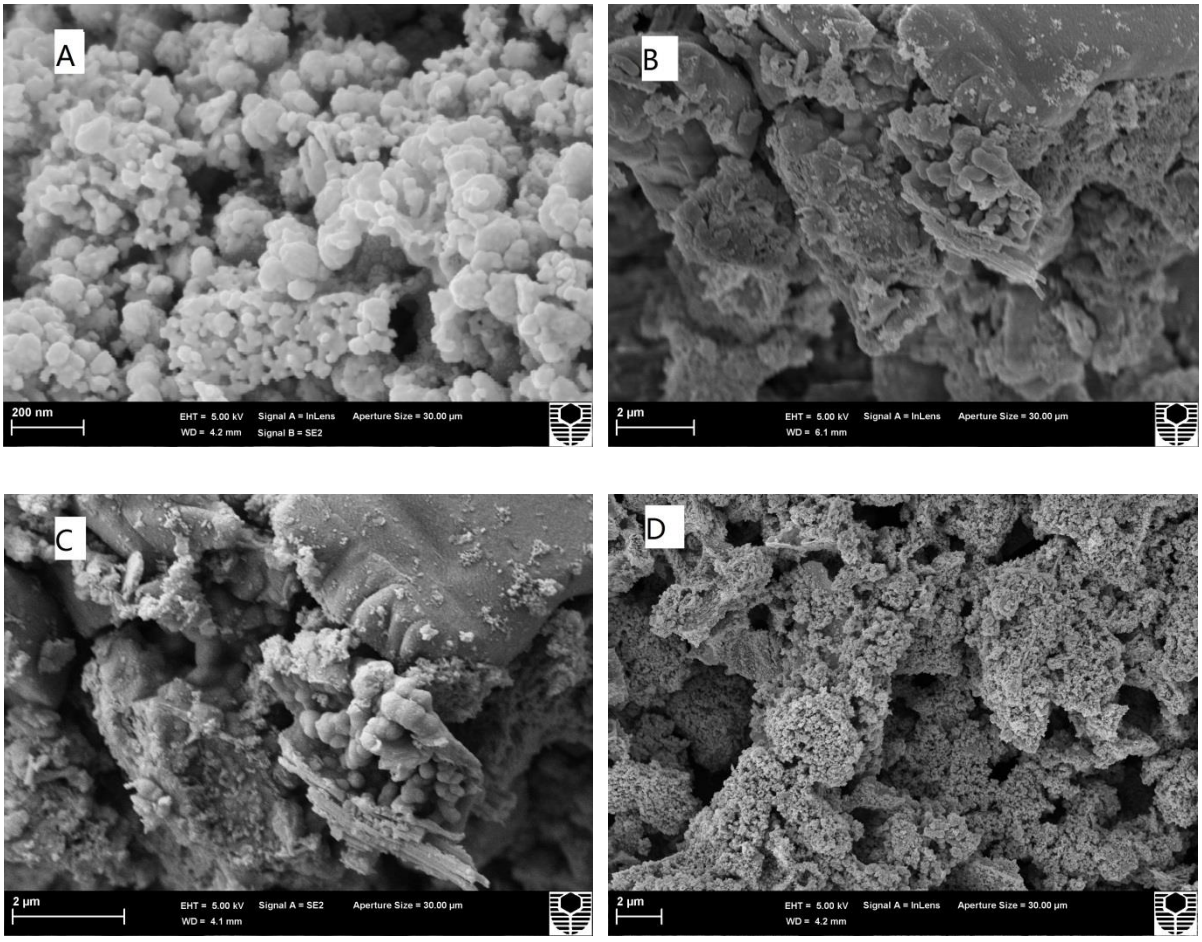

Figure 5.1 SEM images of $Ag_6Si_2O_7$ (A) and g-C_3N_4/$Ag_6Si_2O_7$ composites (B, C, and D).

Figure 5.1 shows SEM images of the synthesized materials. Figure 5.1 (A) shows that the $Ag_6Si_2O_7$ nanoparticles had sphere-like morphology and the particle size is approximately 50 nm. And it also can be seen that the nanoparticles were aggregated, due to the inter-molecular dipolar interaction. Figure 5.1 (B, C and D) shows the morphology of g-C_3N_4/$Ag_6Si_2O_7$ composites that $Ag_6Si_2O_7$ nanoparticles were adhered on the surface of g-C_3N_4.

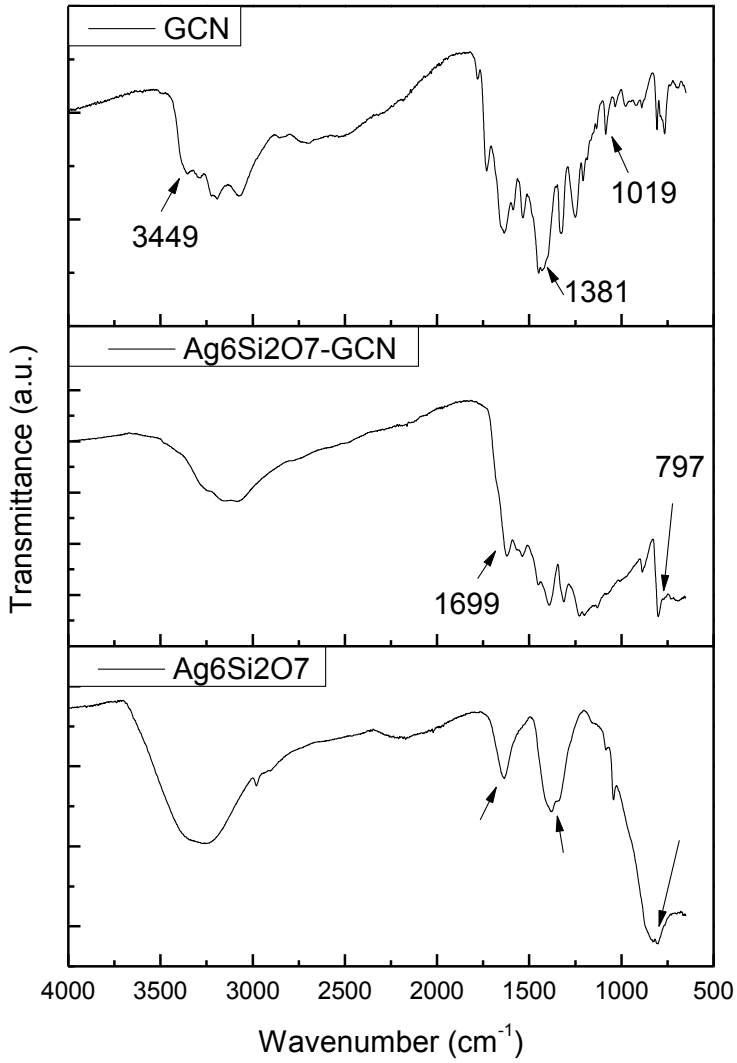

Figure 5.2 FT-IR spectra of g-C_3N_4, $Ag_6Si_2O_7$ and g-C_3N_4/$Ag_6Si_2O_7$-50% composites.

In Figure 5.2, FT-IR spectra are used to evaluate the functional groups of prepared photocatalyst samples. As seen, the strong IR bands at 1381 cm^{-1} and 1699 cm^{-1} were attributed to C-C and C=O vibrations, respectively, and the band at 797 cm^{-1} was due to aromatic C-H bending vibrations. For the $Ag_6Si_2O_7$, which were attributed to Si-Si, Si=O, and Si-H vibrations. All can be found in these three samples. The peaks around 1246 – 1650 cm^{-1} was corresponding to the typical skeletal vibrations of CN heterocycles, which cannot found in the pattern of $Ag_6Si_2O_7$ photocatalyst. The band at 1019 cm^{-1} indicated the presence of

C-O stretching vibrations and a peak at 3449 cm^{-1} was a characteristic signal of –OH vibrations, which only showed in the pattern of pure g-C_3N_4.

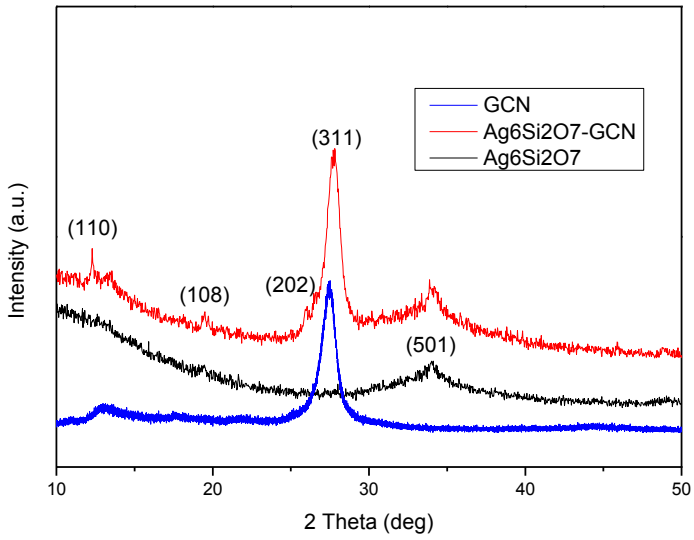

Figure 5.3 XRD patterns of g-C_3N_4, $Ag_6Si_2O_7$, and g-C_3N_4/$Ag_6Si_2O_7$-50% composites.

Figure 5.3 shows XRD patterns of prepared g-C_3N_4, $Ag_6Si_2O_7$, and g-C_3N_4/$Ag_6Si_2O_7$ composites. It can be seen that $Ag_6Si_2O_7$ dopant has some effects on the XRD pattern of g-C_3N_4. Strong g-C_3N_4 and $Ag_6Si_2O_7$ peaks can be found in g-C_3N_4/$Ag_6Si_2O_7$ composites at 27.4° and 34.8°, respectively. Some weak peaks of g-C_3N_4/$Ag_6Si_2O_7$ composites at 10° to 20° were detected in the XRD analysis, corresponding to characteristics peaks of crystal planes of g-C_3N_4 (110) and (108), respectively.

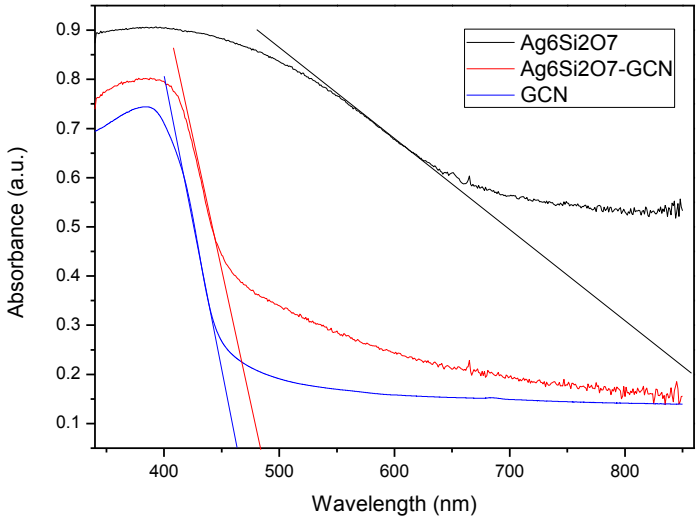

Figure 5.4 Spectra of diffuse reflectance spectroscopy of photocatalysts.

Figure 5.4 shows UV-vis diffuse reflectance spectra of g-C_3N_4, $Ag_6Si_2O_7$, and g-C_3N_4/$Ag_6Si_2O_7$-50% composites. It can be seen that g-C_3N_4, and g-C_3N_4/$Ag_6Si_2O_7$ showed much similar profiles and $Ag_6Si_2O_7$ presented differently. For g-C_3N_4 and g-C_3N_4/$Ag_6Si_2O_7$-50%, a strong broad band centred at around 400 nm. The g-C_3N_4 exhibits absorption onsets at 460 nm, is corresponding to the band gap at 2.63 eV, and the band gap of g-C_3N_4/$Ag_6Si_2O_7$-50% composites is 2.58 eV.

5.3.2 Photocatalytic activity tests

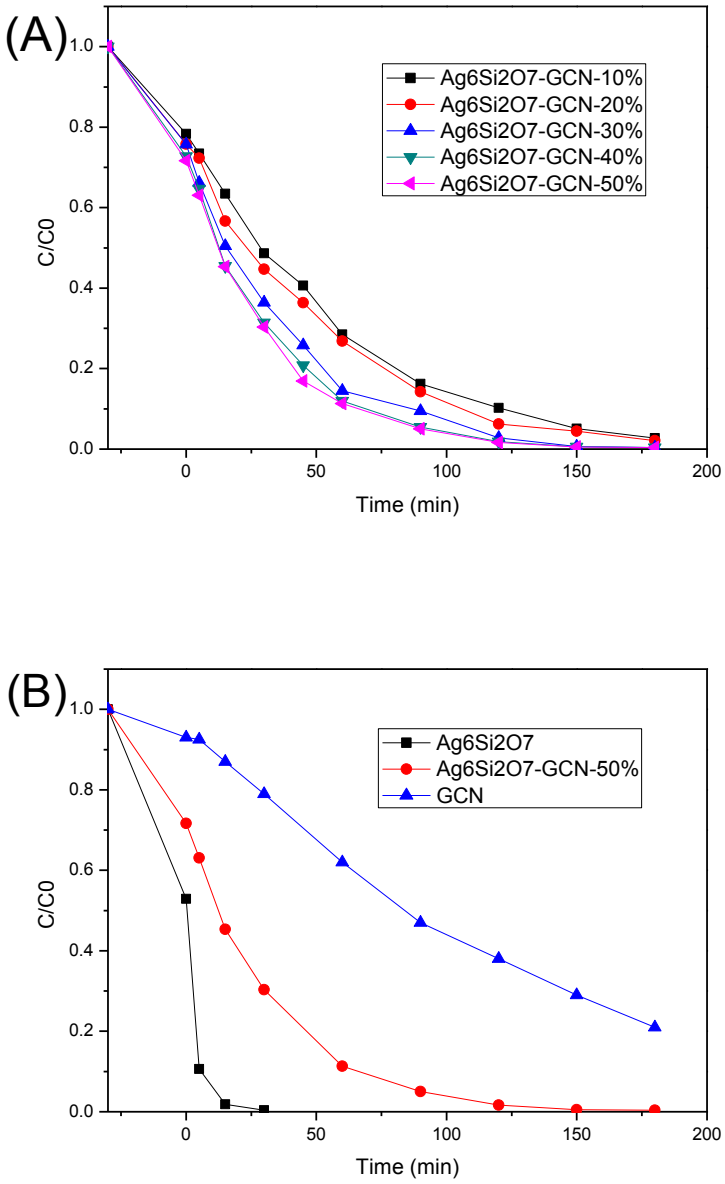

Figure 5.5 Activities of methylene blue decomposition with various ratios of g-C_3N_4/$Ag_6Si_2O_7$ composites (A), g-C_3N_4 and $Ag_6Si_2O_7$ (B) under UV-vis light irradiation.

Figure 5.5 (A) shows that various ratios of g-C_3N_4/$Ag_6Si_2O_7$ composites can make a complete decomposition of methylene blue in 180 min. Among them, the g-C_3N_4/$Ag_6Si_2O_7$ -50% could achieve 100% degradation under 120 min irradiation. It also can be seen from Figure 5.5 (B) that the pure $Ag_6Si_2O_7$ has the greatest photocatalytic activity for methylene blue removal,

which would degrade 100% methylene blue within 30 min. For pure g-C_3N_4, only 20% of methylene blue was degraded at 30 min, and achieved 80% degradation at 180 min under UV-vis light irradiation. However, the adsorption of methylene blue on $Ag_6Si_2O_7$ is also much higher than g-C_3N_4 and g-C_3N_4/$Ag_6Si_2O_7$ composites (see below).

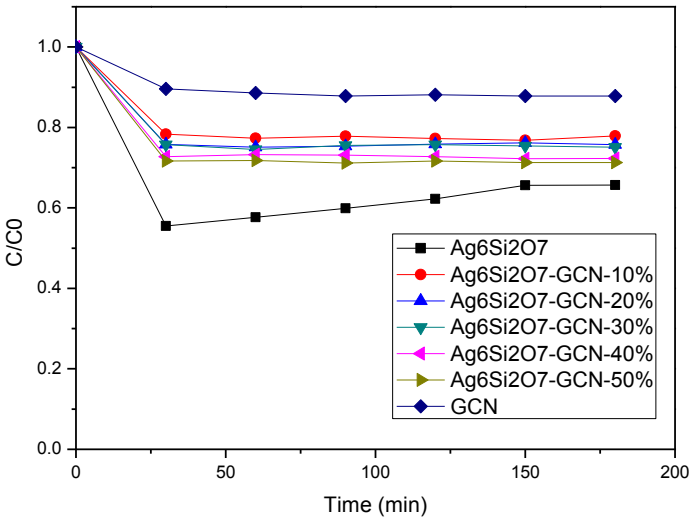

Figure 5.6 Adsorption of MB on photocatalysts in 3 hours.

Figure 5.6 shows the adsorption of methylene blue on the g-C_3N_4, $Ag_6Si_2O_7$ and g-C_3N_4/$Ag_6Si_2O_7$ composites. It was shown that the photocatalysts presented adsorption of methylene blue from 12% to 38% at 180 min, and the adsorption of $Ag_6Si_2O_7$ was much greater than other photocatalysts. Especially at the first 30 min, the adsorption of methylene blue on the $Ag_6Si_2O_7$ was up to 46%. Moreover, the reduction of the methylene blue in the photocatalytic tests was mainly contributed to the photodegradation of photocatalysts.

5.4 Conclusion

The g-C_3N_4/$Ag_6Si_2O_7$ composites were successfully synthesized using a facile hydrolysis and ion-exchange method with different $Ag_6Si_2O_7$ loading ratio in this study. The photocatalytic properties were examined. The g-C_3N_4/$Ag_6Si_2O_7$-50% performed a high photocatalytic

activity in decomposition of methylene blue under UV-vis light irradiations. The modified structure between $Ag_6Si_2O_7$ and g-C_3N_4 contribute to the enhanced photocatalysis.

References

1. Shukla, P., et al., *Co-SBA-15 for heterogeneous oxidation of phenol with sulfate radical for wastewater treatment.* Catalysis Today, 2011. **175**(1): p. 380-385.

2. Gupta, V.K., et al., *Chemical treatment technologies for waste-water recycling-an overview.* RSC Advances, 2012. **2**(16): p. 6380-6388.

3. Christoskova, S.G., M. Stoyanova, and M. Georgieva, *Low-temperature iron-modified cobalt oxide system: Part 2. Catalytic oxidation of phenol in aqueous phase.* Applied Catalysis A: General, 2001. **208**(1–2): p. 243-249.

4. Fortuny, A., et al., *Bimetallic catalysts for continuous catalytic wet air oxidation of phenol.* Journal of Hazardous Materials, 1999. **64**(2): p. 181-193.

5. Calleja, G., et al., *Activity and resistance of iron-containing amorphous, zeolitic and mesostructured materials for wet peroxide oxidation of phenol.* Water Research, 2005. **39**(9): p. 1741-1750.

6. Huang, C.-P. and Y.-H. Huang, *Application of an active immobilized iron oxide with catalytic H2O2 for the mineralization of phenol in a batch photo-fluidized bed reactor.* Applied Catalysis A: General, 2009. **357**(2): p. 135-141.

7. Hoffmann, M.R., et al., *Environmental Applications of Semiconductor Photocatalysis.* Chemical Reviews, 1995. **95**(1): p. 69-96.

8. Linsebigler, A.L., G. Lu, and J.T. Yates, *Photocatalysis on TiO2 Surfaces: Principles, Mechanisms, and Selected Results.* Chemical Reviews, 1995. **95**(3): p. 735-758.

9. Fujishima, A., T.N. Rao, and D.A. Tryk, *Titanium dioxide photocatalysis.* Journal of Photochemistry and Photobiology C: Photochemistry Reviews, 2000. **1**(1): p. 1-21.

10. Zhang, J., et al., *Co-Monomer Control of Carbon Nitride Semiconductors to Optimize Hydrogen Evolution with Visible Light.* Angewandte Chemie International Edition, 2012. **51**(13): p. 3183-3187.

11. Maeda, K., et al., *Photocatalytic Activities of Graphitic Carbon Nitride Powder for Water Reduction and Oxidation under Visible Light.* The Journal of Physical Chemistry C, 2009. **113**(12): p. 4940-4947.

12. Zhang, X., et al., *Enhanced Photoresponsive Ultrathin Graphitic-Phase C3N4 Nanosheets for Bioimaging.* Journal of the American Chemical Society, 2012. **135**(1): p. 18-21.

13. Zheng, Y., et al., *Graphitic carbon nitride materials: controllable synthesis and applications in fuel cells and photocatalysis.* Energy & Environmental Science, 2012. **5**(5): p. 6717-6731.

14. Bejblová, M., D. Procházková, and J. Čejka, *Acylation Reactions over Zeolites and Mesoporous Catalysts.* ChemSusChem, 2009. **2**(6): p. 486-499.

15. Lou, Z., et al., *Ag6Si2O7: a Silicate Photocatalyst for the Visible Region.* Chemistry of Materials, 2014. **26**(13): p. 3873-3875.

6

Chapter 6: Conclusions and future work

6.1 Concluding comments

The major objective of this research is to synthesize novel graphitic carbon nitride based photocatalysts to degrade organic compounds in aqueous phase via UV-light irradiation. Graphitic carbon nitride (g-C_3N_4) was synthesized by a facile thermal treatment of melamine. Various types of modified graphitic carbon nitride photocatalysts were synthesized with hydrothermal method or hydrolysis and ion-exchange method, and used for decomposition of methylene blue solution with UV-vis light irradiation. Metal-oxide doped graphitic carbon nitride (Fe_2O_3-g-C_3N_4, Fe_3O_4-g-C_3N_4 and MnO_2-g-C_3N_4) photocatalysts were synthesized by a hydrothermal method. Polyometalate nanoparticles (POMs) were also synthesized by a hydrothermal method and used to modify g-C_3N_4. G-C_3N_4/$Ag_6Si_2O_7$ composites were synthesized using a facile hydrolysis and ion-exchange method. All these catalyst materials were tested for methylene blue photocomposition under UV-vis light irradiation. Some of these catalysts were also investigated for activating peroxymonosulfate (PMS) for the degradation of phenol.

6.2 Effect of metal-oxide doped graphitic carbon nitride

A series of metal-oxide doped graphitic carbon nitride have been successfully prepared by a facile hydrothermal method. The physical and optical properties of g-C_3N_4 have changed upon metal deposition, and the large heterojunction interface and intrinsically layered structure of MnO_2-g-C_3N_4 could enhance methylene blue decomposition process.

6.3 One step synthesis of polymetalate modified g-C_3N_4

Polymetalate modified g-C_3N_4 photocatalysts have been successfully synthesized via a one-step hydrothermal method. The structures and photocatalytic properties of g-C_3N_4 have been improved. PMo_{12}@g-C_3N_4 photocatalysts exhibited a better efficiency in degradation of methylene blue and phenol under UV-vis light irradiation.

6.4 Photocatalytic activities of silicate modified g-C_3N_4

Silicate modified graphitic carbon nitride catalysts (g-C_3N_4/$Ag_6Si_2O_7$ composites) were synthesized using a facile hydrolysis and ion-exchange method. The g-C_3N_4/$Ag_6Si_2O_7$ composites showed an excellent photocatalytic activity in decomposition of methylene blue under UV-vis light irradiations and relatively low adsorption of methylene blue.

6.5 Scope for future work

This research focused on the modification of graphitic carbon nitride photocatalyst for degradation of methylene blue or phenol in aqueous phase under UV-vis light irradiation. The results demonstrated that methylene blue can be decomposed into by-products via various catalysts under illumination. However, the catalysts need to be examined for other organic pollutants. And it also needs to conduct the tests of the catalysts with other oxidants, such as hydrogen peroxide and potassium permanganate.

In this study, the focus was to explore the photocatalytic activity of catalysts for methylene blue oxidation reaction. However, further study on the stability of the catalysts and the mechanism of photocatalysis needs to be done to investigate by-products and intermediates, which may cause the secondary pollution in water treatment processes.

Our investigation showed that photocatalysis of methylene blue conducted in a batch process has been achieved. However, in order to employ this technology to industrial scale, detailed testing route on a continuous process needs to be done to investigate various parameters such as flow rate of feeding, time of residence, and kinetic constants.